THE ASEAN JOURNAL OF RADIOLOGY

May - August 2010
Volume XVI Number II
ISSN 0859 144X

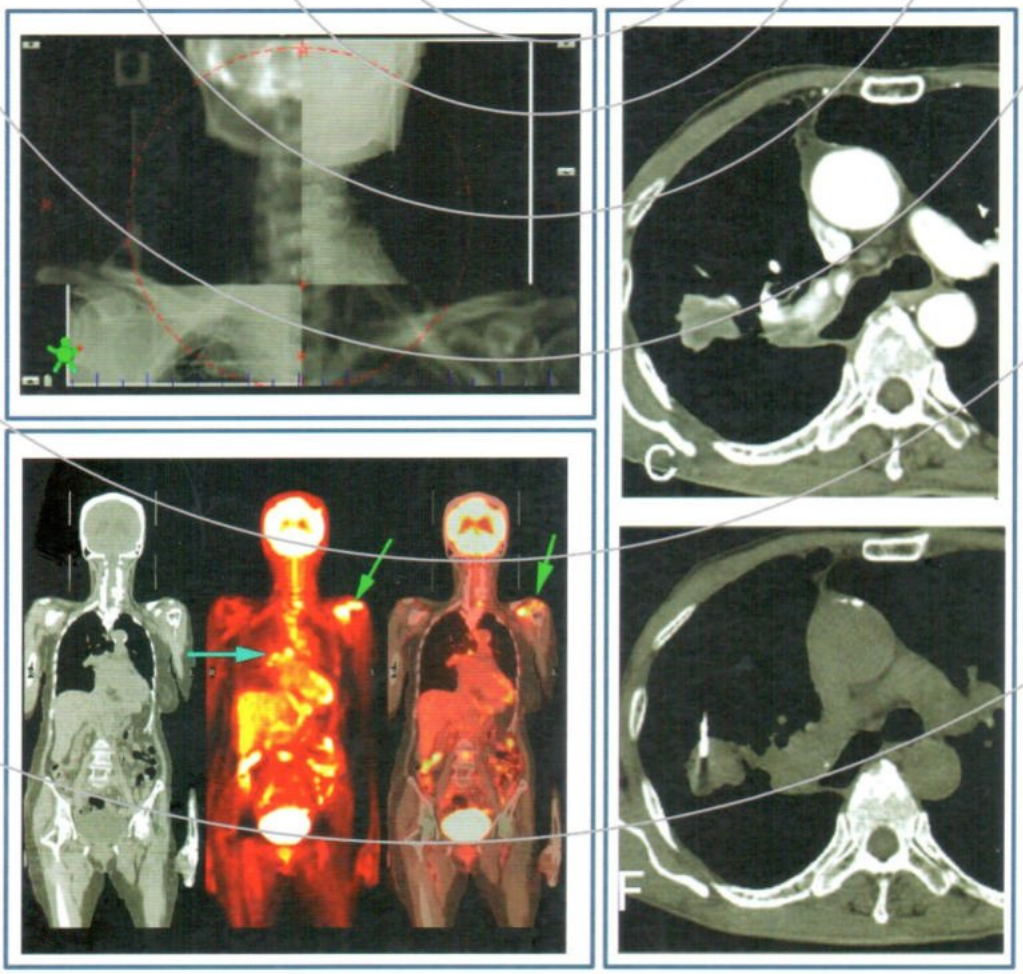

Published by

Royal College of Radiologists of Thailand

and

Radiological Society of Thailand

Bangkok, Thailand.

Mae-Ya waterfall
นพ.ไพฑูรณ์ วิชิวานิเวศน์

Paithoon Wichiwaniwate
Lens Sigma 10-20, Nikon 70-300 VR

THE ASEAN JOURNAL OF RADIOLOGY
May-August 2010, Volume XVI No.II

The Committee of Royal College of Radiologists of Thailand

Apr 2009- Mar 2011

President:	Permyot	Kosolbhand
Vice-president:	Yongyut	Kongthanarat
Secretariat General:	Poonsook	Jitnuson
Vice-secretary General:	Pongdej	Pongsuwan
Treasurer:	Krisdee	Prabhasavat
Academic president:	Sirintara	Singhara Na Ayudya
House Master&Social Programme:	Chutakiat	Kruatrachue
Secretary:	Piyaporn	Apisarnthanarak
Registrar:	Alongkorn	Kiatdilokrath
Committee:	Chorfa	Kaewjinda
	Pimjai	Siriwongpairat
	Chamaree	Chuapatcharasopon
	Pisit	Wattanaruangkowit

The Committee of Radiological Society of Thailand

Apr 2009- Mar 2011

President:	Permyot	Kosolbhand
Vice-president:	Yongyut	Kongthanarat
Secretariat General:	Poonsook	Jitnuson
Treasurer:	Krisdee	Prabhasavat
Academic president:	Amphai	Uraiverotchanakorn
House Master&Social Programme:	Chutakiat	Kruatrachue
Secretary:	Piyaporn	Apisarnthanarak
Committee:	Chorfa	Kaewjinda
	Chamaree	Chuapatcharasopon
	Alongkorn	Kiatdilokrath
	Pisit	Wattanaruangkowit
	Surat	Vinijsorn

The Journal of the Royal College of Radiologists & Radiological Society of Thailand

(2009 - 2011)

Office:

1. Department of Radiology, Faculty of medicine, Ramathibodi hospital 270, Rama VI Road, Toong Phayathai, Ratchathewi, Bangkok, 10400.
   Tel 02-201-1259 #110, Fax 02-201-1297, E-mail Sirintarapongpech2@hotmail.com
2. The Royal college of Radiologists & Radiological society of Thailand. 9th Floor, Royal Golden Jubilee Building, 2 Soi Soonvijai, Petchburi Road, Bankok, 10320
   Tel 02-716-5963, Fax 02-716-5964, E-mail rcrtthailand@gmail.com

Contents

Original Article

Case Report

THE ASEAN JOURNAL OF RADIOLOGY 2010; 16(2): 83-90 83

Original Article

Entrance Surface Dose in Intravenous Pyelography Patients at Songklanagarin Hospital

Anchali Krisanachinda, Ph.D.[1], Seri Sakjirapapong, B.Sc.[2]
Thamanoon Viriyabubpha, B.Sc.[2], Amporn Funsian, M.Sc.[2]

[1]Department of Radiology, Faculty of Medicine, Chulalongkorn University

[2]Department of Radiology, Faculty of Medicine, Prince of Songkla University

Abstract

The purposes of the study are to determine of entrance surface dose and the dose reference level from Intravenous Pyelography patients during April-July 2008 at Songklanagarind Hospital. The doses were calculated at the patient skin from 121 patients in 7 radiographic routine projections: scout IVP AP view, 5 min after contrast media injection, 10 min prone, 10 min supine, 30 min, full bladder and post voiding. The results showed the mean /third quartile entrance skin doses, using as the dose reference level at this center, for the 7 projections of 1.90/2.10, 2.93/3.47, 1.72/2.00, 2.22/2.68, 2.39/2.76, 2.99/3.44 and 2.25/2.70 mGy respectively. Most of the dose levels were generally within normal range of the diagnostic reference levels specified by European Commission as the European Guidelines for KUB studies of 10 mGy for entrance surface dose of a standard sized patient. However, there was one record with over normal range value caused by improper radiographic exposure technique.

Key Word: entrance surface dose, intravenous pyelography, radiographic projection

Introduction

The optimal use of ionizing radiation involves the interplay of three important aspects of the imaging process:

1. The diagnostic quality of the radiographic image,
2. The radiation dose to the patient,
3. The choice of radiographic technique.

In order to meet the optimization in patient, the European Commission[1] (EC) had set up The European Guidelines on Quality Criteria for Diagnostic Radiographic Images. This contains the Quality Criteria for six conventional examinations: Chest, Skull, Pelvis, Lumbar Spine, Urinary Tract and Breast. It defines diagnostic requirement for a normal, basic radiograph, specifying anatomical image criteria and important image details; it indicates criteria for the radiation dose to European Guidelines on Quality Criteria for diagnostic radiographic images.

As the routine intravenous pyelography (IVP) radiographic examination consists of seven projections of

1. Scout IVP
2. Five minutes after contrast media injection
3. Ten minutes after injection, supine projection
4. Ten minutes after injection, prone projection
5. Thirty minutes after injection
6. Full Urinary Bladder
7. Urinary Bladder Post voiding

Special care is taken during x-ray examinations to use the lowest radiation dose possible while producing the best images for evaluation. National and international radiology protection councils continually review and update the technique standards used by radiology professionals.

Quality Criteria for Diagnostic Radiographic Images[2] - KUB

1. Diagnostic requirements - Image criteria

1.1 Reproduction of the area of the whole urinary tract from the upper pole of the kidney to the base of the bladder

1.2 Reproduction of the kidney outlines

1.3 Visualization of the psoas outlines

1.4 Visually sharp reproduction of the bones

2. Important image details:

calcifications of 1.0 mm

3. Good Radiographic Technique

3.1 Radiographic device: grid table

3.2 Nominal focal spot value: 1.3 mm

3.3 Total filtration: 1.3 mm Al equivalent

3.4 Anti-scatter grid: r = 10; 40/cm

3.5 Screen film system: nominal speed class 400

3.6 FFD: 115 (100-150) cm

3.7 Radiographic voltage: 75-90 kV

3.8 Automatic exposure control: chamber selected - central or lateral

3.9 Exposure time: < 200 ms

3.10 Protective shielding: where appropriate, gonad shields should be employed for male and female patients.

- AP Projection

Either as plain film or before or after administration of contrast medium

Remarks: Compression is usually indicated. Satisfactory reduction of overlying bowel gas and faeces is essential for adequate urinary tract reproduction.

4. Diagnostic requirements- function criteria

Image criteria are to be referred to a series of

radiographs, taken at intervals after contrast administration, tailored to the individual patient.

4.1. Increase in parenchymal density (nephrographic effect)

4.2. Visually sharp reproduction of the renal pelvis and calyces (pyelographic effect)

4.3. Reproduction of the pelvic-ureteric junction

4.4. Visualization of the area normally traversed by the ureter

4.5. Reproduction of the whole bladder area

5. Important image details

5.1. Calyceal detail: 0.3 mm

5.2. Calcifications: 1.0 mm

Criteria for Radiation dose to the Patient

Entrance surface dose for a standard-sized patient is 10 mGy per radiograph

1. Dose Monitoring

Prior to patient dose assessment, the information on x-ray exposure parameters (kVp, mAs) and geometrical parameters- X-ray tube focus film distance (FFD), X-ray tube focus-to-skin distance (FSD), field size in X-ray examinations of adult patients of average body mass for selected X-ray projections were collected. The X-ray exposure parameters were used later to estimate patient doses through a four step protocols: X-ray tube output measurement, incident air-kerma measurements, the entrance skin air-kerma (ESAK) calculations and entrance skin dose (ESD) determinations.

Materials

1. X-ray system. Manufacturer Quantum Model VZW2930 RC 2-82 (Fig 1A)
2. Solid state detector manufacturer UNFORS Model Xi (Fig 1B)
3. Special ruler for patient thickness measurement

Methods

1. Perform the quality control of the radiographic system using AAPM protocols for kVp accuracy and mGy/mAs test.
2. Patient data collection:

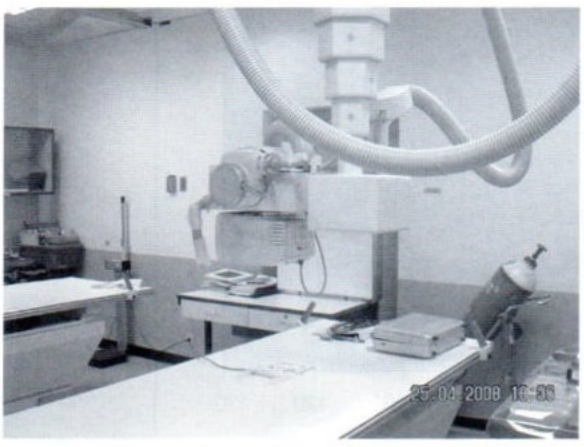

(A)

Fig.1A Radiographic system for IVP procedure.

(B)

Fig.1B Solid state dosemeter for air kerma measurements

2.1 H.N.

2.2 Age, weight, height, body thickness, gender

2.3 Patient dose determination

2.3.1 Record the following parameters: kVp, mA, FDD, FFD, exposure times.

2.3.2 Calculate the patient entrance skin dose, ESD

$$ESD = Y(kVp, FDD) \cdot mAs \cdot \left[\frac{FDD}{FDD\text{-}t_p}\right]^2 \cdot BSF$$

Y(kVp, FDD) is tube output for actual *kVp* used during examination (taken from output chart), *mAs* is actual tube current-time product used during examination and *FFD* is focus-to-film distance, while *FDD* is focus-detector distance and t_p is the patient thickness. BSF is the backscatter factor that depends on kVp and total filtration of X rays.

Results

1. The kVp accuracy and the relationship with mGy/mAs determination. The set kVp and measured kVp are accepted as they were within 10 percent. The relationship between the set kVp and mGy/mAs is displayed in fig. 2 as the output in air, air kerma, at the particular distance. The solid state detector is placed in air as the geometry in fig. 3 showing the distance of FFD and FDD.

2. Patient characteristics. Number of patients is 121 as information in table 1.

Discussion

The 121 patients underwent IVP in the year 2008 at Department of Radiology, Songklanagarind Hospital were 51 males and 70 females. The

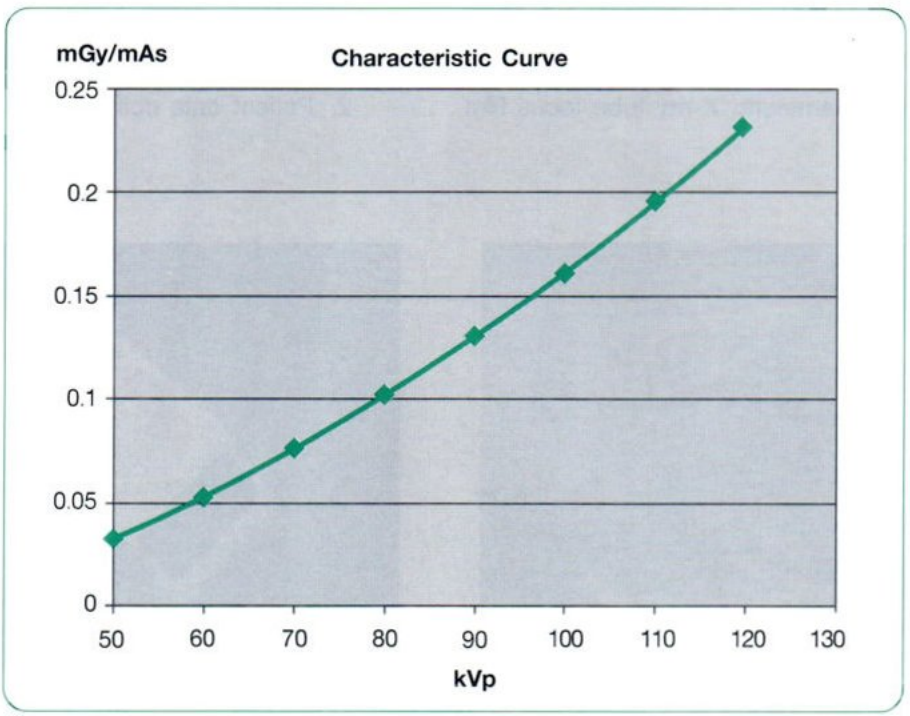

Fig.2 The linear relation between kVp and mGy/mAs

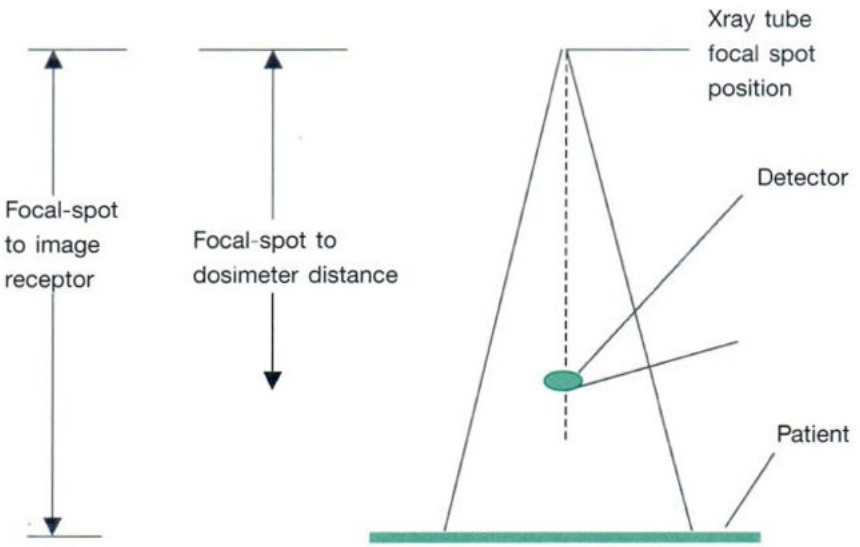

Fig.3 Geometry used for X- ray output measurements

Table 1 The information from 121 patients who underwent IVP at Songklanagarind Hospital

Gender		Age (years)			Weight (kg)			Height (cm)			BMI (kg.m^{-2})		
Male	Female	Ave	Min	Ma	Ave	Min	Max	Ave	Min	Max	Ave	Min	Max
51	70	54	20	80	65	43	96	163	148	180	24.45	15.76	33.6

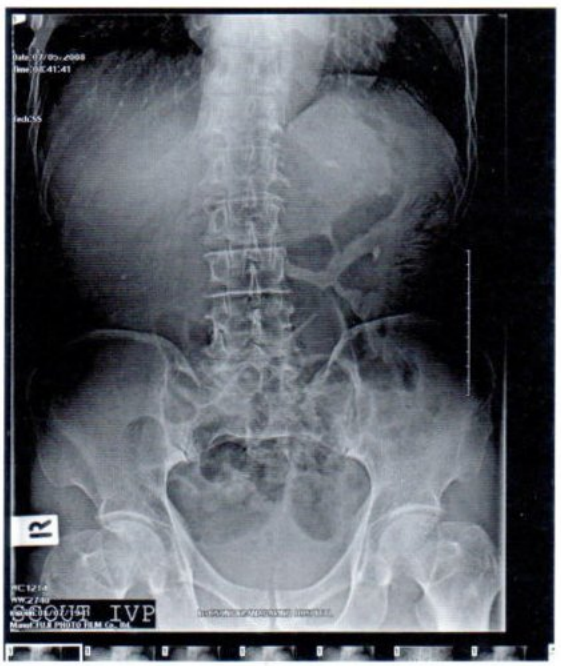

Fig.3 An X-ray image during IVP procedure

images were taken for each projection as the exam in fig.3. The age range was 20-80 years old, the weight was 43-96 kg, the height 148-180 kg and the body mass index was 15.76-33.60 kg.m^{-2}. The average entrance surface dose for all 7 projections was 1.90-2.99 mGy. The maximum ESD was recorded at projection 6 of urinary bladder of 11.84 mGy which exceeded the Dose Reference Level of 10 mGy per projection. The third quartile per projection was calculated and range was 2.0-3.47 mGy. Those values were much less than the DRL of 10 mGy. The scatter plot on body thickness and ESD showed the poor relation between both parameters. The ESD increases as the body thickness increases. The urinary bladder received the

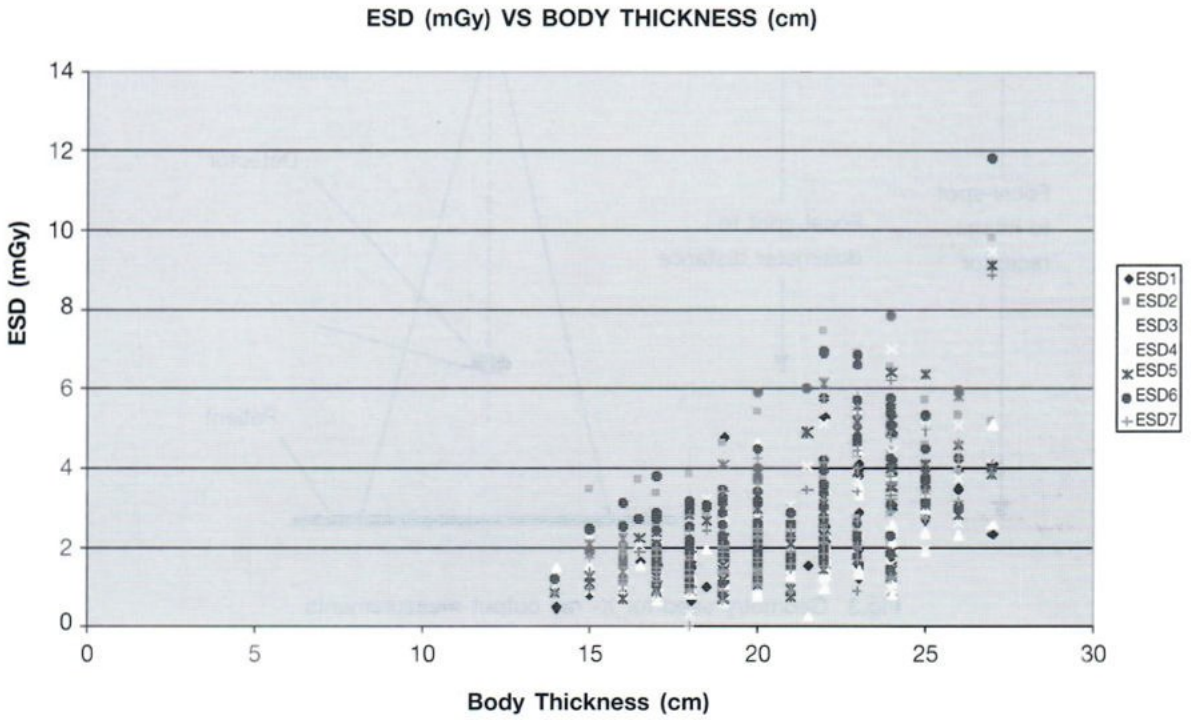

Fig.4 The correlation between the patient skin dose (mGy), ESD and body thickness (cm)

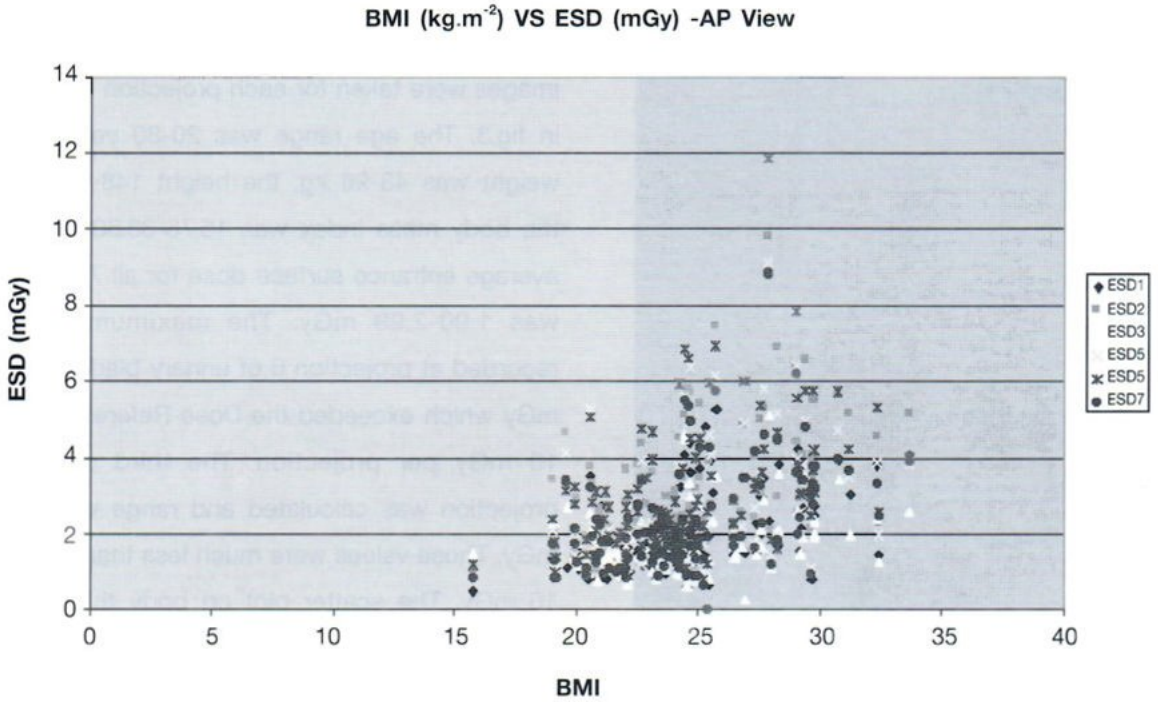

Fig.5 The relation between the patient skin dose of 7 projections (ESD, mGy) and the Body Mass Index ($kg.m^{-2}$)

Table 2 The calculated entrance skin dose for 7 projections as the average, minimum and maximum values in mGy

	kVp	ESD1	ESD2	ESD3	ESD4	ESD5	ESD6	ESD7
Ave	81	1.90	2.93	1.72	2.22	2.39	2.99	2.25
Min	72	0.51	0.96	0.29	0.32	0.71	0.80	0.66
Max	88	5.30	9.82	5.13	9.47	9.12	11.84	8.85
3rd quartile		2.10	3.47	2.0	2.68	2.76	3.44	2.70

highest ESD of 11.84 mGy and the body thickness at the pelvis was 27 cm. as in fig.4. The relation between the body mass index and the entrance surface dose was shown in fig.5 of the scatter plot of increasing BMI resulted in the increasing ESD. The ESD from projection 1, scout view, and patient number was shown in bar graph as in fig.6.

Conclusion

An intravenous pyelogram (IVP) is an x-ray examination of the kidneys, ureters and urinary bladder that uses iodinated contrast material injected into veins. State-of-the-art x-ray systems have tightly controlled x-ray beams with significant filtration and dose control methods to minimize stray or scatter

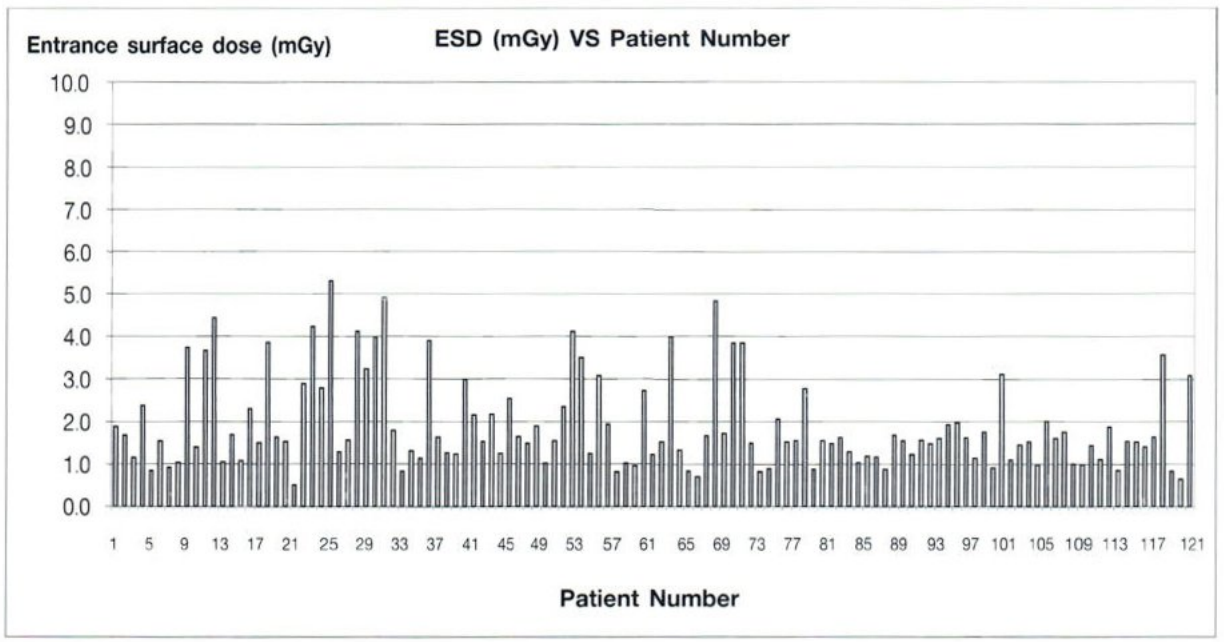

Fig.6 The bar graph of ESD (mGy) of scout view projection with the patient number.

radiation. This ensures that those parts of a patient's body not being imaged receive minimal radiation exposure.

Generally, the effective radiation dose from this procedure is about 1.6 mSv[3], which is about the same as the average person receives from background radiation in six months. From our study, the effective dose is only 0.38 mSv for the average ESD of 7 projections which is about a quarter of the international dose value.

The survey on the status of image quality and radiation dose to patients in IVP examination forms an important component of a quality assurance program. Knowledge of the image quality and patient dose level, as well as reasons behind poor quality and higher doses, provide a basis for setting corrective actions in order to optimize the protection of the patient in an effective manner. Patients expected to be informed about clinical risks including radiation risks 4,5 hence another aspect of the usefulness of patient dose data. The determination of the ESD and the DRL are the important part of the optimization process in diagnostic radiology.

References

1. IAEA. International Conference (IAEA/EC/PAHO/WHO). Developing and Using Dose Guidance Level in Radiology and Nuclear Medicine Examinations Contributed papers. 2001:403-87.
2. European Commission. European Guidelines on Quality Criteria for Diagnostic Radiographic Images. EUR 16260 EN 1996.
3. Muhogora W, Nada AH, Aziz A, Alsuwaidi J, Beganovic A, Ciraj-Bjelic O, Kabuya FK, Krisanachinda A, Milakovic M, Rehani MM. Patient doses in radiographic examinations in 12 countries in Asia, Africa and Eastern Europe - Initial results from IAEA Projects. IAEA TEC DOC 2006.
4. Faulkner K. Topics for research and development in the radiological protection of patients. IN: Proceedings of International Conference 26-30 March 2001, Malaga., Vienna 2001:379-88.
5. Balaban B, Marshall-Depommier E, Ferraro F. Expectations of patients' advocates. IN: Proceedings of International Conference 26-30 March 2001, Malaga., Vienna 2001:379-88.

THE ASEAN JOURNAL OF RADIOLOGY 2010; 16(2): 91-100 91

Original Article

Emergency Transcatheter Arterial Embolization in Ruptured Hepatocellular Carcinoma in Siriraj Hospital

Chutakiat Kruatrachue, MD., Krisdee Prabhasavat, MD., Narumon Jarunsap, MD., Patcharin Prapaisilp, M.Sc.

Department of Radiology, Siriraj Hospital, Mahidol University, Bangkok, Thailand 10700

Abstract

Objective: To review the outcome of the patients who had ruptured hepatocellular carcinoma after receiving TAE and to identify prognostic indicators in Siriraj Hospital

Patient and Method: Retrospectively reviewed the outcome of patients who had undergone TAE for rupture of HCC during March 2003 - December 2006,. Angiographic finding, arterial embolization, size of tumor, tumor location, agents used for embolization were recorded. The final outcome in terms of technical success, 0-3 day clinical success, 30 days mortality rate, overall mean survival time and complication were recorded. Correlation between portal vein patency with incidence of liver failure was calculated. We also compared their survival time in each child-Pugh classification and with respect to different prognostic indicators.

Results: Adult: 35 men and 3 women. (ranges 17-89 years and mean age 53.11 years. At the time of ruptured tumor) 2 patients had Child's A, 13 Child's B and 23 of Child's C disease. The most common presentation was abdominal pain (17 patients). Bleeding was successfully immediate arrested in all 38 patients. The most tumor location was detected at right lobe of liver (20 patients). The overall mean survival was 61.92 days. We found that survival time between Child B and C classification had statistically significant difference. Twenty four patients died within 30 days after TAE, the major cause of death was liver failure, which occurred in 7 patients. In addition, we had also postulated several prognostic indicators for patients' survival. The results showed that only those with a bilirubin level more than 3 mg/dl had a poor outcome. (P=0.05)

Conclusion: TAE should be considered in management of patients with ruptured HCC. It is effective in arresting tumor bleeding. Patients who are considered poor surgical candidates with Child B or C hepatic cirrhosis might have emergency embolization as a life-saving measure. Failure TAE is not depends on only technique but also depends on underlying disease and general condition prior embolization.

Introduction

Hepatocellular carcinoma (HCC) is a disease with a high prevalence rate in South East Asia due to the high incidence of hepatitis associated cirrhosis. The clinical presentation can be varied. Patients may present with jaundice, weight loss, and abdominal mass or abdominal pain. Others may be asymptomatic and picked up incidentally on routine screening for carriers of the hepatitis virus. Also, it is not uncommon to have spontaneous rupture of a tumor as the initial presentation. In the Far East, the rupture rate is as high as 10%, while in Hong Kong the rupture rate is around 9.7%.[1-4] without any treatment, the outcome is poor and survival rate is only 10%. Ruptured HCC is the major life-threatening complication. Traditionally, surgeons operate on those patients who present with ruptured HCC and the treatment is varied, consisting of packing, hepatic artery ligation and hepatectomy. However, surgery is often associated with a high mortality rate; the latter has been reported to be as high as 70%.[2-4] Therefore, a relatively less invasive procedure should be considered for patients with rupture of HCC and transcatheter hepatic arterial embolization (TAE) is gaining popularity in this area. The purpose of our retrospective study was to determine technical and outcome of patients who underwent TAE that we achieved in 3 years in Department of Radiology, Siriraj hospital.

Material and Method

Patients' selection

Medical records of patients with ruptured HCC who had undergone TAE during March 2003 - December 2006, were retrospectively reviewed and the outcome was analyzed. Informed consent for embo-lization was obtained from all conscious patients. This retrospective study was approved by the Ethics Committee of our hospital.

The diagnosis of ruptured HCC was based on two major criterias:

(1) clinical presentation of acute abdominal pain, distension, hypotension or shock.

(2) radiological findings of a liver tumor with evidence of bleeding - either frank hemoperitoneum or a subcapsular hematoma.

All of the patients who underwent TAE also was confirmed with ultrasound, non-contrast-enhanced CT, dual-phase CT or abdominal paracentesis, or combinations of any of these modalities before transcatheter arterial embolization.

Sex, age, clinical presentation, laboratory data and Child-Pugh classification were recorded in each patient.

Informed consent for embolization was also obtained.

Modality for work up ruptured hepatocellular carcinoma :-

- Abdominal paracentesis: blood-stained ascites or unclotted blood.

- Ultrasonography (US): High echoic area localized around tumor

- Computed tomography (CT) scan: Useful in detecting HCC rupture by showing tumor, by defining the extent of the hematoma, and by showing serial density changes with the age of the hematoma. The hyperdensity of acute hematoma is best visualized on noncontrast CT.

Optimal CT protocol for this condition triphasic phase:-

- Precontrast phase allows for assessment of hematoma. Arterial phase demonstrates enhancement of the mass. Portal venous phase allows for assessment of the portal veins.

CT Features of ruptured hepatocellular carcinoma:

(1) Discontinuity of the hepatic surface
(2) Active extravasations of contrast
(3) Subcapsular hematoma
(4) Presence of a sentinel clot
(5) Extra hepatic hematoma with high attenuation
(6) Marked ascites or hemoperitoneum
(7) Subtle rim enhancement (enucleation sign)
(8) Densely enhancing peripheral rim with marginal break.

Angiography: hyper vascular with tumor staining mass, extravasations of contrast medium and aneurysm.

Time from onset to angiography, amount of blood for resuscitation before angiography, baseline hemoglobin were recorded.

Intervention data were analyzed as follow:

Angiographic finding; Extravasations, hyper vascular with tumor staining and vascular abnormality such as aneurysm.

Arterial embolization; RHA, LHA and both or accessory RHA or others size of tumor and tumor location.

The agents used for embolization were basically gelfoam, stainless steel coils or polyvinyl alcohol sponge (Ivalon); the choice was primarily depending on the size of the artery being embolized and the radiologists' preference. In general, gelfoam was the preferred option, as the arteries could be recanalized providing an opportunity of further chemoembolization.

Immediately following embolization, hepatic arteriogram was repeated to ascertain the success of hemostasis.

The catheter for selection; 5 Fr Cobra, 5 Fr Yashiro catheter, Simm1 catheter, 5 Fr Shepherd Hook catheters and coaxial micro catheter were used.

Patients were monitored closely for any signs of rebleeding and complications, which included liver failure, fever, abdominal pain and wound problems. If patients had clinical sign of rebleeding, doctor will referred for surgery or repeat angiography with embolization.

Data analysis

Angiographic diagnosis and embolization technical success rate were analyzed by one interventional radiologist (experience > 15 yrs). Technical success means the result of embolization immediately after the intervention. 30-day mortality rate mean rate of number of patients who died within 30 day.

For the survival time period, we had follow-up the patients until death or until the end of the study observation time. (31 March 2007)

The final outcomes were analyzed as follow;

- Technical success, 0-3 day clinical success, 30days mortality rate, complication and survival time.
- Technical success (bleeding target devascularization) was assessed the result immediately after embolization, if immediate follow up arteriography showed devascularization of target vascular lesion or disappearance of extravasations, success was considered.
- They were divided in two types: partial and complete success.
- The complete success was defined as disappearance of extravasations or significant devascularized target vascular lesion.
- The partial success was defined as remaining minimal extravasations.

- 0-3 day clinical success was observation period to detect therapy-related failures.

- If patient had died or rebleeding, 0-3 day clinical unsuccess was considered.

- Rebleeding was described as unstable vital sign or no response to PRC or IV fluid or shock during resuscitation.

- Hematologic parameters (Hb) were serially followed up. Follow up imaging was reevaluated when clinical was indicated.

- In all patients, hemorrhage ceased almost immediately after embolization, as confirmed by the occlusion of feeding arteries of tumors, normalization of blood pressure and stabilization of hemoglobin levels.

- 30 days mortality rate was calculated for evaluate after treatment within 30 days and review most common cause.

- Complications were analyzed such as low grade fever, right upper quadrant or epigastric pain, liver failure or other.

- Correlation between portal vein thromboses with liver failure was calculated.

- The overall mean survival rate and mean survival of each Child-Pugh were calculated.

- Moreover, we also compared the survival of patients with respect to different possible prognostic indicators by using the survival Kaplan-Meier survival curves. Statistical significance was defined as $p \leq 0.05$.

Statistical analysis

SPSS statistical software version 11.5. Descriptive statistic analysis: report with frequency and percentage. Kaplan Meier curve for survival time in respect to prognostic factor.

Results

From March 2003 - December 2006, there were 54 patients who underwent TACE.16 cases were excluded due to not available film and medical record. 38 patients with spontaneous ruptured HCC were retrospectively reviewed. Altogether, there were 35 men and 3 women in our study aged 17-89 years with a mean age of 53.11 years. (Table 1).

Clinical presentation :The most patients presented with sudden onset of abdominal pain (44.7%) and distension (42.2%). (Table 1) Most of patient was sent to angiography within 24 hrs from initial symptom.

On admission, most of patients had hemoglobin < 8 g/dl and received blood transfusion in 2 units before angiography. 2 patients had Child A liver cirrhosis, 13 Child B and 23 Child C disease. (Table 1 (continued))

Location of tumor: The most common location of tumor was right lobe of liver (52.6%) (fig.1-2). Left lobe and bilobes were 5.3 and 42.1%, respectively. The right hepatic artery was selected in 25 patients (65.8%). The left hepatic, both of them and accessory right hepatic arteries were selected in 4, 3 and 6 patients, respectively. (Table 1 (continued))

Tumor size: The size of the HCC was determined on ultrasound or CT and ranged from 4.0 to 23.0 cm in maximum diameter. All embolizations were performed via the femoral approach. The 5 Fr catheters were used in 28 patients (73.7%). The other such as Yashiro, Simm[1], Shepherd and micro catheter were also used.

Angiographic findings:The most angiographic findings seen in our study was hyper vascular with tumor staining in 22 patients (56.4%). Extravasations and aneurysm were demonstrated in 14 and 2 patients, respectively. (Table 2 and fig.3-8).

Table 1 Patient demographic data and bleeding parameters

Parameter	Number of Patients (Percentage)
Sex	
Male : Female	35 (92.1) : 3 (7.9)
Age group (y) Mean age = 53 years	
≤ 20: 21-60 : 61-80 : > 80	1 (2.6) : 27 (71.1):9(23.7): 1 (2.6)
Presentation	
Abdominal pain	17 (44.7)
Abdominal distention	16 (42.2)
Abdominal pain with shock	4 (10.5)
Abdominal distention with Hct drop	1 (2.6)
Time from onset to angiography (day)	
< 1 : 1-3: 3-6: ≥ 7	16 (42.1) : 11 (28.9): 5 (13.2): 6 (15.8)
Hb (g/dl)	
< 8 : 8-10: ≥ 10	17 (44.7) : 12 (31.6): 9 (23.7)
Blood transfusion (units)	
0 : 1-2: 3-4: >4	6 (15.8) : 27(71): 4(10.6): 1 (2.6)
Child-Pugh classification	
A : B: C	2 (5.3) : 13 (34.2): 23 (60.5)
Location	
RL : LL : Both lobes	20 (52.6) : 2 (5.3): 16 (42.1)
Arterial embolization	
RHA : LHA: Both: Accessory RHA	25 (65.8) : 4 (10.5): 3 (7.9): 6 (15.8)

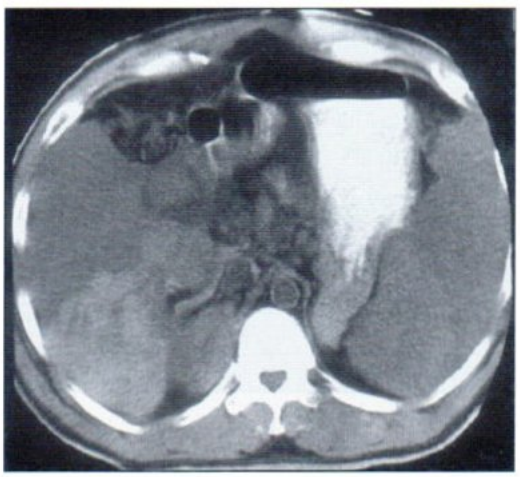

1.

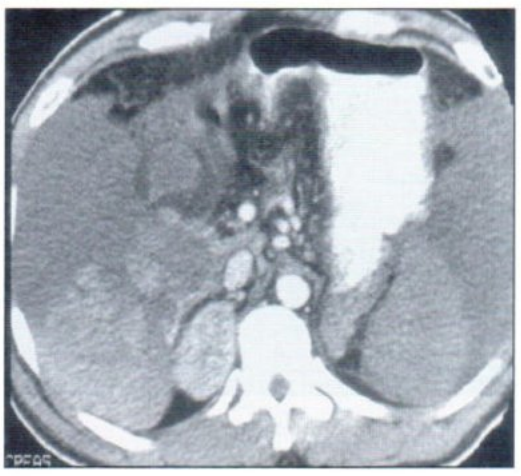

2.

Fig.1 and 2 Noncontrast and contrast-enhanced CT show enhancing ill-defined mass at segment 5 of right lobe liver. Large amount of ascites was noted.

There were hepatoportal shunt in 8 pts and hepatohepatic shunt in 1 pt. There were main portal vein thromboses in 14 pts (36.8%), right portal vein thrombosis in 16 pts (42.1%) and left portal vein thrombosis in 13 pts (34.2%). (Table 2).

Gelfoam pledget about 1-2 mm. were used in

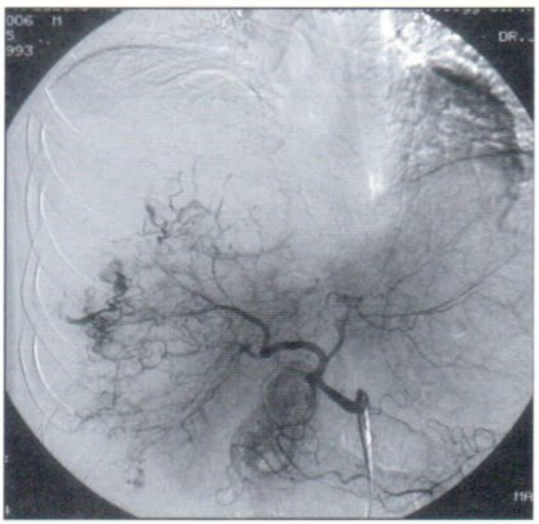

3.

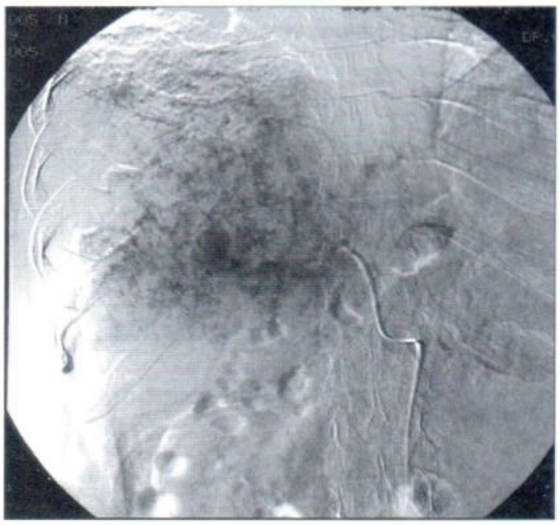

4.

Fig. 3 Angiogram showed extravasations of contrast medium at inferior aspect of right lobe liver. Medial displacement of liver is noted which could be due to large amount of ascites or hemoperitoneum.

Fig. 4 Angiogram showed hypervascular mass with tumor staining scattered in the entire right lobe liver.

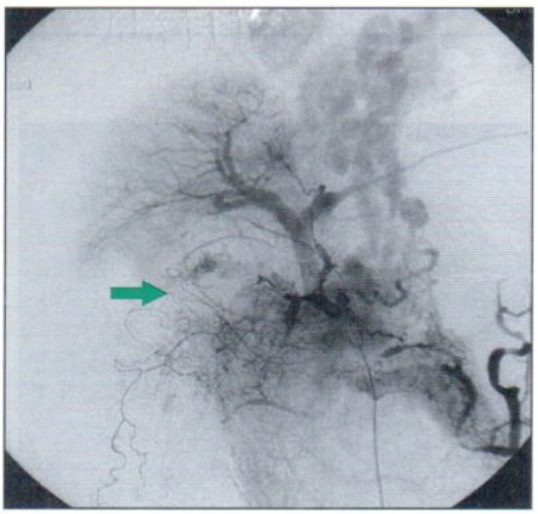

5.

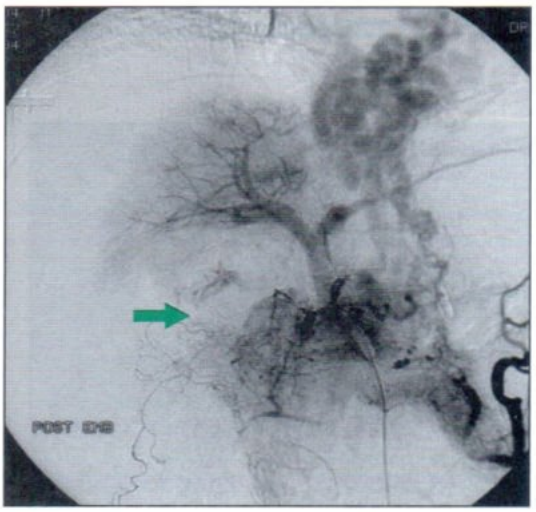

6.

Fig. 5 Preembolization showed extravasations of contrast medium at segment 5. Paraesophageal varices are also noted.

Fig. 6 Postembolization showed remaining of minimal extravasations of contrast medium. On 6 hours later, he developed hypotension and no response to blood replacement. The patient died within 24 hours later.

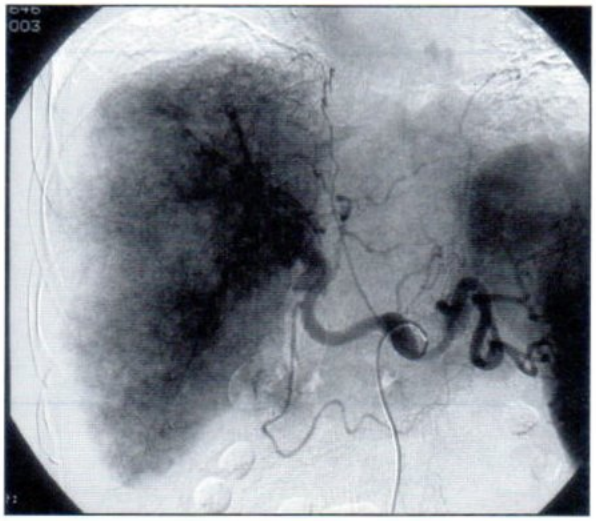

7.

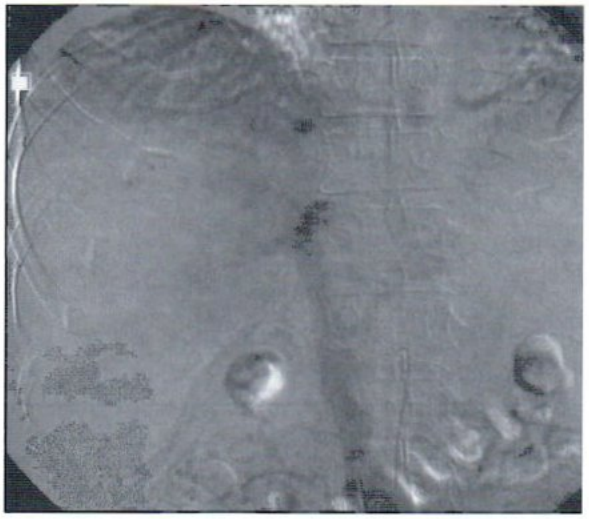

8.

Fig.7 and 8 Hepatic angiogram showed diffuse hypervascular masses with main and right portal vein thrombosis. After TAE, liver enzyme rising was demonstrated. 11 days later, he died due to liver failure

every cases. Additional Lipiodol in four cases were performed. (Table 3)

After TAE, bleeding was arrested in all 38 patients, which was confirmed by the post TAE arteriogram

Clinical outcome:The technical success rate of embolization was achieved in all 38 patients (100%). Complete technical success rate of embolization was 34 patients (89.5%) Partial technical success rate that mean partial decreased vascularity of the target vascular lesion or minimal contrast material extravasations was in 4 patients (10.5%). (Table 4).

Early 3-day Failure. 76.3% (29 of 38 patients) who underwent technically successful embolization had no clinical evidence of reruptured tumor within 3 days. While early failure rate was 23.7% (9 of 38 patients) and 30 days mortality rate is 63.2% (24 of 38 patients). (Table 4)

From days 1-3 after embolization, two patients had re-ruptured tumor and one of cases died on day 2 and another case was followed by explore laparotomy and discharge later, while three cases of partial success angiogram died within 24 hrs, three cases experienced liver failure and died within 3 days and one case died within 3 days due to pneumonia and renal failure. (Table 4)

Apart from liver failure in seven patients (29%), which was the major cause of death during admission, three patients had partial success of angiography, six patients died from underlying medical condition, two patients developed re-ruptured without resuscitation or other treatment, and six patients died at home and outside hospital. (Table 5).

Overall mean survival time and mean survival for each child classification. The overall mean survival time of those after TAE was 61.92 days. Mean

Table 2 Angiographic findings

Findings	Number (n=38)	Percentage
Extravasations	14	36.8
Hyper vascular with tumor staining	22	56.4
Pseudo aneurysm	2	5.1
Main portal vein thrombosis	14	36.8
Right portal vein thrombosis	16	42.1
Left portal vein thrombosis	13	34.2
Hepatoportal shunt	8	21
Hepatohepatic shunt	1	2.6

Table 3 Embolic agents

Embolic agents	Number (n=38)	Percentage
Gel foam : Gel foam+Lipiodol: Glue	34 : 4 : 0	89.5 : 10.5 : 0

Table 4 Clinical outcome

Outcome	Yes Number of Patients (Percentage)	No Number of Patients (Percentage)
Technical success (n=38)	38 (100) - complete = 34(89.5), - partial = 4 (10.5)	0 (0)
0-3 days clinical success	29 (76.3)	9 (23.7)
30 days clinical success	14 (36.8%)	24 (63.2%)

Table 5 0-3 days failure rate (n=9) (23.7%)

Cause	Number	Percentage
Liver failure	3	33.33%
Re-rupture	2	22.22%
Partial success of angiographic finding with suspected rebleeding (survival <24 hrs)	3	33.33%
Multifactor	1	11.11%

**8 cases death within 3 days

*1 case - rebleed with follow by explore lap and discharge later

Table 6 Survival in each Child-Pugh classification

Child pugh	Survival period (months)					Mean
	0-1	1-3	3-6	6-12	>12	survival(days)
A: B : C	0: 7 :17	1: 2 : 6	0: 3 : 0	0: 1 : 0	1: 0 : 0	521.5: 66.9: 19

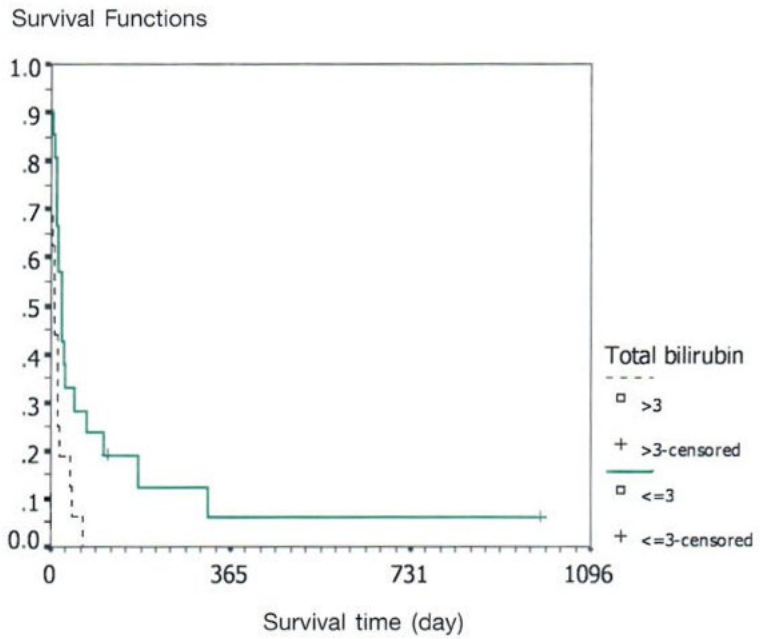

Fig. 9 Cumulative survival curves of patients having serum total bilirubin level above or below 3 mg/dl.

survival period of child A was 521.5 days, Child B was 66.9 days and Child C was 19 days. (Table 6)

Complications: The most common complication after procedure was fever in seven patients and liver failure in seven pts. Other complication, five patients complained of right upper quadrant or epigastric pain, six patients did not have any postembolization symptoms, one patient experienced hematoma at right groin and one patient experienced chill on perioperation.

The significant prognostic factor was the level of bilirubin. Those with a bilirubin level more than 3 mg/dl had a mean survival of 21 days, whereas those patients with a level less than 3 mg/dl had a mean survival of 115days (P=0.05). (fig.9)

The other prognostic factors; age > 60 or tumor size did not alter the outcome in terms of life expectancy. (fig.9)

Conclusion

TAE should be considered in the management of patients with ruptured HCC It is effective in arresting tumor bleeding. Patients who are considered poor surgical candidates with Child's B or C hepatic cirrhosis might have emergency embolization as a life-saving measure. However, the proce-

dure should be done selectively as not all the patients will benefit from this intervention. Failure TAE is not depends on only technique but also depend on underlying disease and general condition prior embolization.

References

1. Hirai K, Kawazoe Y, Yamashita K, Kumagai M. Transcatheter arterial embolization for spontaneous rupture of hepatocellular carcinoma. Am J Gastro 1986;81, No.4: 275-9.
2. Dewar GA, Griffin SM, Ku KW, Lau WY, et al Management of bleeding liver tumor in Hong Kong Br J Surg 1991;78:463-6.
3. Miyamoto M, Sudo T and Kuyama T. Spontaneous rupture of hepatocellular carcinoma: a review of 172 Japanese cases. Am J Gastro 1991;86:67-71.
4. Zhu LX, Wang GS and S Fan ST. Spontaneous rupture of hepatocellular carcinoma. Br J Surg 1996;83(5):602-7.
5. Kim P, Su J, et al Computed Tomography and Angiographic Interventional Features of Ruptured Hepatocellular Carcinoma: Pictorial Essay CARJ Vol 57, No 3, June 2006.
6. Nagasue N, Iuokuchi K. Spontaneous and traumatic rupture of hepatoma. J Surg 1979;66:248-50.
7. Okazaki M, Higashihara H, Koganemaru F, et al Intraperitoneal hemorrhage from hepatocellular carcinoma: emergency chemoembolization or embolization. Radiology 1991;180:647-51.
8. Hsieh JS, Huang CJ, Huang YS, Sheen PC, Huang TJ. Intraperitoneal hemorrhage due to spontaneous rupture of hepatocellular carcinoma: treatment by hepatic artery embolization. AJR 1987;149:715-17.
9. Ngan H, Tso WK, Lai CL, Fan ST. The role of hepatic arterial embolization in the treatment of spontaneous rupture of hepatocellular carcinoma. Clin Radiol 1998; 53:338-41.
10. Sato Y, Fujiwara K, Furui S, et al. Benefit of transcatheter arterial embolization for ruptured hepatocellular carcinoma complicating liver cirrhosis. Gastroenterology 1985;89: 157-9.
11. Shiina S, Ibukuro K. Transcatheter arterial embolization for the treatment of ruptured hepatocellular carcinoma. AJR 1989;153:658-9.
12. Leung C, Tang C, Fung K, et al A retrospective review of transcatheter hepatic arterial embolisation for ruptured hepatocellular carcinoma, journal of royal collage of surgeon of Edinburgh, October 2002 Volume 47 Number 5.

THE ASEAN JOURNAL OF RADIOLOGY 2010; 16(2): 101-107 101

Original Article

Reproducibility of the Patient Setup for Head and Neck Cancers using On-Board Imager System

Wilai Masa-Nga, B.Sc., Natchayaporn Thonapan, B.Sc., Sawanee Suntiwong, B.Sc., Kittipol Dachaworakol, B.Sc., Sangutid Thongsawat, M.Sc., Chirasak Khamfongkhruea, B.Sc., Pittayapoom Pattaranutraporn, MD., Chirapha Tannanonta, M.Sc.

Division of Radiation Oncology, Chulabhorn Hospital, Bangkok, Thailand

Abstract

Objective: To study the setup error of patient positioning in head and neck cancer with customized thermoplastic long mask using On-Board Imager (OBI) system.

Materials and Methods: This study is a retrospective analysis of the setup error data from June 2008 to February 2009. The data were collected from 12 head and neck cancer patients with IMRT technique using the thermoplastic long mask for 6 MV photon beams. Two images in AP (anterior-posterior) and lateral views were taken with the On-Board Imager mounted on the gantry of the linear accelerator machine before treating the patient. Then these images were matched with the DRR (Digital Radiographic Reconstruction) images of planning CT by using the OBI software to determine the setup errors in vertical (anterior-posterior), longitudinal (superior-inferior), and lateral (left-right) directions.

Results: From 187 sessions of the matching, the mean values of setup error were 0.19 ± 0.18 cm, 0.21 ± 0.18 cm, and 0.11 ± 0.11 cm for vertical (Vrt), longitudinal (Lng), and lateral (Lat) directions respectively. The maximum setup errors were 0.9 cm, 0.6 cm, and 0.5 cm for Vrt, Lng, and Lat directions from two patients with cutting thermoplastic long mask at the port and neck regions. For normal masks, the maximum values were 0.5 cm, 0.5 cm, and -0.5 cm for Vrt, Lng, and Lat directions.

Conclusion: All setup errors in head and neck cancer of this study are acceptable for thermoplastic long mask without cutting. The OBI system is shown to be useful for reducing the uncertainty of interfraction and increasing the efficiency of radiation therapy.

Key words: Evaluation, Setup error, On-Board Imager, head and neck cancer.

Introduction

In the process of radiation therapy, patient's positioning and immobilization are important because the error may result in the rate of tumor control and patient complication. The optimized radiotherapy is to deliver maximum dose to the tumor and minimum dose to the critical normal tissue. Especially in head and neck cancer, the accuracy of radiation dose to target volume is required due to the proximity of many critical structures such as brain stem, spinal cord, and parotid glands. So reproducibility of the patient positioning is particularly important for increasing the efficiency of radiation treatment.

There are many verification devices that can be used to check the patient's position before treatment such as port film[1], EPID (Electronic portal imaging)[2,3], and kV or MV On-Board Imager (OBI)[4,5]. The kV on-board imager was used in this study. It is qualified to take high quality image, reduce radiation dose to patient, have automated matching software which can automatically shift the couch to the correct position.

Fox et al[6] studied the performance of image registration software and repositioning a 3D offset using OBI software. Verification tests were performed to assess the precision and accuracy of the automated positioning system in a known offset phantom. They found that the average deviation between detected and known offset was less than 0.75 mm. Their conclusion is the precision and accuracy of OBI system checkup daily, setup error margin can be reduced to less than 1.4 mm.

Mechalakos et al[7] performed the measurement of interfraction and intrafraction setup deviations for head and neck cancer patients using a kV OBI. They summarized that the systematic errors were seen in the interfractional data, but not in the intrafractional data, indicating that the mask is better at maintain head position than reproducing it.

Pahlivan et al[8] assessed interfractional setup errors from daily electronic portal images in twenty head and neck cancer patients with a fixed 5 point mask immobilization system. The systematic setup errors were less than 1 mm in the three directions whereas the random setup errors were around 2 mm.

This study was designed to evaluate the setup error of the patient positioning in head and neck cancer with customized thermoplastic long mask using kV On-Board Imager system.

Materials and Methods

This study is a retrospective analysis of the setup error data in 12 head and neck cancer patients treated with IMRT (Intensity modulated radiation therapy) technique, by using 6 MV photon beams from a Varian linear accelerator (Trilogy®, Varian Medical System, Palo, Alto) at Radiation Oncology Division, Chulabhorn Cancer Centre. The data was collected from June, 2008 to February, 2009. All patients were immobilized with a thermoplastic long mask (TYPE-S™) covering head, neck, and shoulder but two of them were cut for patient comfortable as shown in Fig.1. (a) and (b) respectively. The mask was fixed to the couch of the treatment machine. At the treatment couch, the patients were setup by using lasers aligned to skin markers on the mask. Orthogonal verification images (anterior-posterior and lateral) were taken with the kV On-Board Imaging device permanently mounted on the gantry of the linear accelerator machine. Then both images were matched with the DRRs (Digitally Reconstructed Radiographs) from planning CT by using the OBI software.

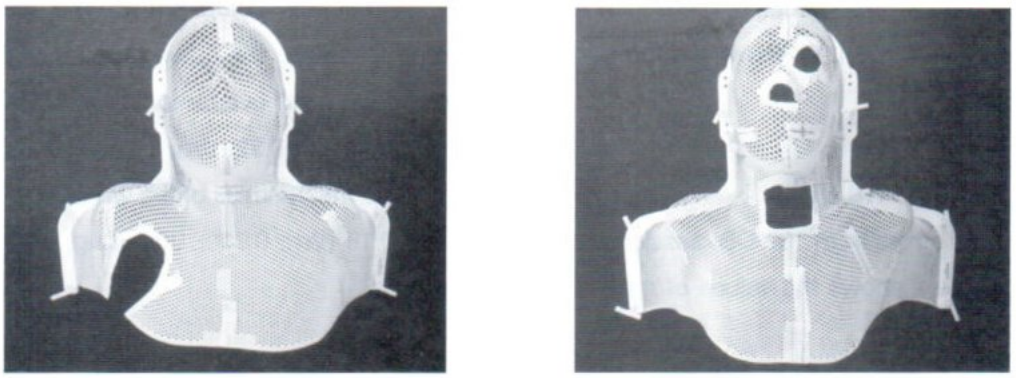

(a) (b)

Fig.1 The thermoplastic long masks with cutting parts. (a) at the port area and (b) at the neck, nose and eye area.

Image analysis

The OBI and reference images were overlaid in gray scale and aligned by using auto-matching software then manual matching of bony anatomy drawn on the reference images. For the first fraction, the alignment was evaluated by the oncologist. Fig.2 shows the OBI console of matching result with Split Window.

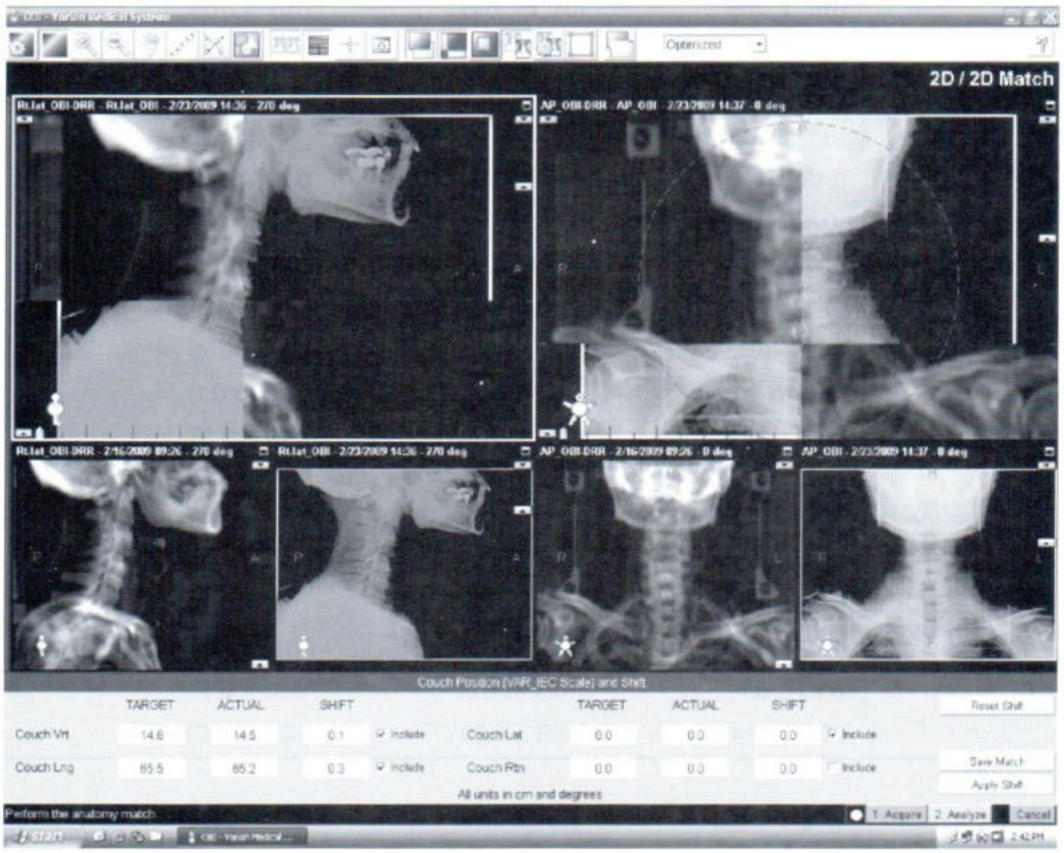

Fig.2 OBI console showing overlaid images and couch shift (error) values.

The shifted or error values of the couch for all directions (Vrt, Lng and Lat) shown on the console were recorded.

Results

The setup errors from 187 OBI sessions were evaluated. Table 1 shows the values of mean ± SD of interfractional setup errors. The patients no. 1 and no. 2 having the cutting masks at the port and neck, nose and eye area present the maximum errors of 0.48 ± 0.22 (Vrt), 0.42 ± 0.08 (Lng) respectively. The mean errors of the whole population were 0.19 ± 0.18 (Vrt), 0.21 ± 0.18 (Lng) and 0.11 ± 0.11 (Lat).

Table 1 The values of mean ± SD, minimum and maximum of interfractional setup errors

Patient No.	Mean ± SD of individual patient setup error			No. of OBI
	Vrt.	Lng.	Lat.	
1	0.48 ± 0.22	(0.0 to 0.9)	0.40 ± 0.16	27
	(0.0 to 0.6)	0.10 ± 0.10	(-0.3 to /0.0)	
2	0.10 ± 0.10	(-0.4 to 0.1)	0.42 ± 0.08	29
	(0.3 to 0.6)	0.05 ± 0.06	(-0.1 to 0.1)	
3	0.14 ± 0.11	(-0.3 to 0.3)	0.04 ± 0.06	15
	(0.1 to 0.2)	0.13 ± 0.10	(-0.2 to 0.3)	
4	0.07 ± 0.08	(0.0 to 0.2)	0.07 ± 0.05	6
	(-0.1 to 0.1)	0.12 ± 0.10	(0.0 to 0.3)	
5	0.13 ± 0.05	(0.1 to 0.2)	0.18 ± 0.10	4
	(0.1 to 0.3)	0.03 ± 0.05	(-0.1 to 0.0)	
6	0.13 ± 0.08	(-0.1 to 0.3)	0.08 ± 0.08	6
	(-0.2 to /0.0)	0.08 ± 0.10	(-0.2 to 0.0)	
7	0.12 ± 0.11	(0.0 to 0.3)	0.22 ± 0.11	5
	(0.1 to 0.4)	0.10 ± 0.07	(-0.2 to /0.0)	
8	0.04 ± 0.05	(-0.1 to 0.0)	0.04 ± 0.05	5
	(-0.1 to 0.1)	0.08 ± 0.08	(-0.2 to 0.1)	
9	0.16 ± 0.12	(-0.4 to 0.3)	0.10 ± 0.10	21
	(-0.3 to 0.3)	0.12 ± 0.10	(-0.4 to 0.0)	
10	0.14 ± 0.13	(-0.3 to 0.2)	0.11 ± 0.08	27
	(-0.3 to 0.2)	0.16 ± 0.15	(-0.3 to 0.3)	
11	0.22 ± 0.14	(-0.4 to 0.5)	0.19 ± 0.15	22
	(-0.3 to 0.5)	0.15 ± 0.11	(-0.2 to /0.4)	
12	0.15 ± 0.11	(-0.3 to 0.3)	0.20 ± 0.17	20
	(-0.5 to 0.4)	0.09 ± 0.09	(-0.3 to 0.2)	
Mean ± SD for the whole population	0.19 ± 0.18	0.21 ± 0.18	0.11 ± 0.11	187

If only the patients with complete masks were taken into account, the mean errors of the three directions would be decreased to 0.13 ± 0.05 (Vrt), 0.12 ± 0.07 (Lng) and 0.11± 0.04 (Lat).

From the scatter plots of the setup errors in AP and lateral views (Fig. 3 a and b), it would seem to appear that the errors were more in Lng+ (cranial) and Vrt+ (anterior) directions.

Table 2 illustrates the number of OBI sessions for each range of errors and also in the percentage of all sessions for head and neck cancer patients. The results show the errors within 0.5 cm with 93%.

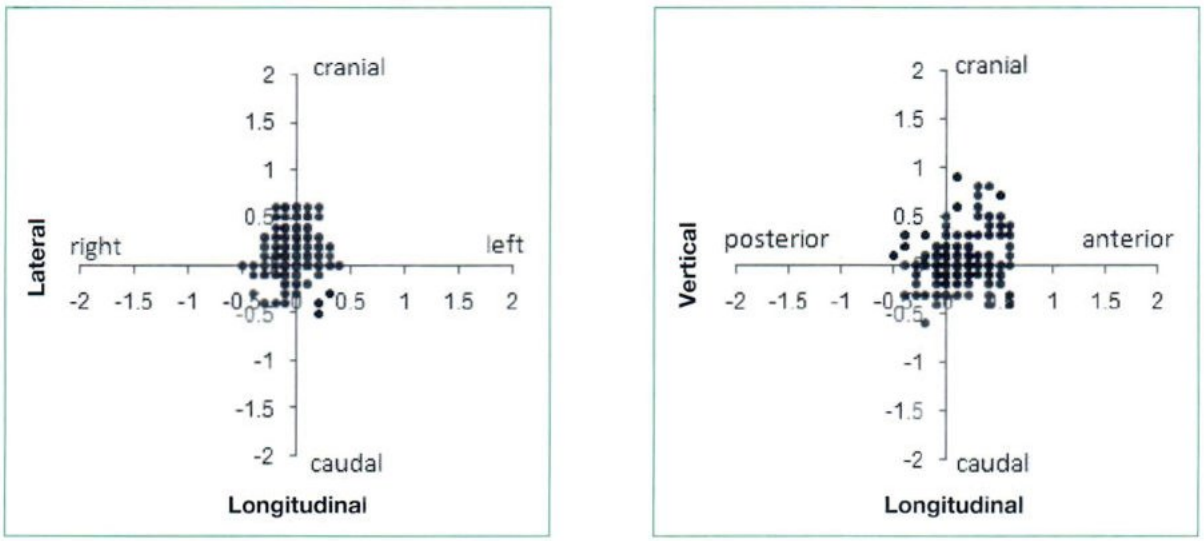

(a) (b)

Fig. 3 Scatter plots of the setup errors for all head and neck patients in anterior-posterior image (a) and lateral image (b).

Table 2 Setup errors of the couch position along the three directions (Vrt, Lng and Lat) for head and neck cancer patients.

Range of setup error (cm)	Frequency		
	Vrt	Lng	Lat
0 - 0.1	105 (56%)	89 (47%)	134 (72%)
0.2 - 0.3	56 (30%)	50 (27%)	48 (25%)
0.4 - 0.5	14 (7%)	39 (21%)	5 (3%)
0.6 - 0.7	9 (5%)	9 (5%)	0 (0%)
0.8 - 0.9	3 (2%)	0 (0%)	0 (0%)
Total	187 (100%)	187 (100%)	187 (100%)

95%, and 100% for anterior-posterior (Vrt), superior-inferior (Lng), and left-right (Lat) directions respectively. The maximum errors were 0.9 cm, 0.6 cm, and 0.5 cm for Vrt, Lng and Lat directions in two patients with cutting thermoplastic long masks.

Discussion

With the OBI unit attached to the treatment machine, the patient images taken before treatment are used to estimate the setup errors by comparing with the standard images from the treatment planning. From the setup errors in the three directions, Vrt, Lng, and Lat evaluated by the OBI software, the couch positions can be automatically shifted to the right values.

According to this study, the setup errors were within 0.5 cm with the maximum mean value of 0.22 cm in all couch directions with the complete masks (no cutting area) which are acceptable for the conventional treatment. Our results are preferable than the study of Fox et al (6) (average deviation = 0.75 mm) and comparable with the study of Mechalakos et al (7) that report the mean values of -0.1 ± 0.3 cm, -0.2 ± 0.3 cm, and 0.0 ± 0.2 cm and Pehlivan et al[8] that propose the mean value of 0.2 cm. The setup error values with 0.9 cm and 0.6 cm for Vrt. and Lng. directions respectively were recorded for 2 patients with the cutting masks, one at the port region and another one at the neck, nose and eye. The error increased and direction of increase depend on the location and size of the cutting region.

Conclusion

From our study, it can be concluded that the long thermoplastic mask is very useful in reproducibility of patient setup or reducing the uncertainty of interfraction for head and neck cancer patient. If the mask has to be cut, the setup error may be up to 1 cm, so the larger PTV has to be considered. The OBI system is shown to be very beneficial that the patient will be treated with very close position to the planning which will increase the tumor control probability and decrease complication rate of the patient especially when the tumor is very close to critical organs and a cutting mask is used.

References

1. Valicenti RK, Michalski JM, Bosch WR, Gerber R, Graham MV, Cheng A, et al. Is weekly port filming adequate for verifying patient position in modern radiation therapy? Int J Radiat Oncol Biol Phys 1994;30:431-8.
2. Boyer AL, Antonuk L, Fenster A, Van Herk M, Meertens H, Munro P, et al. A review of electronic portal imaging devices (EPIDs). Med Phys 1992;19:1-16.
3. Michalski JM, Graham MV, Bosch WR, Wong J, Gerber RL, Cheng A, et al. Prospective clinical evaluation of an electronic portal imaging device. Int J Radiat Oncol Biol Phys 1996;34:943-51.
4. Gilbeau L, Octave-Prignot M, Loncol T, Renard L, Scalliet P, Gregoire V. Comparison of setup accuracy of three different thermoplastic masks for the treatment of brain and head and neck tumors. Radiother Oncol 2001;58: 155-62.
5. Harmon J, Ufflen DV, Laarue S. Assessment of a radiotherapy patient cranial immobilization device using daily on-board kilovoltage imaging. Veterinary Radiology & Ultrasound 2008;50:230-4.
6. Fox T, Huntzinger C, Johnstone P, Ogunleye T, Elder E. Performance evaluation of an automated image registration algorithm using an integrated kilovoltage imaging and guidance system. J Appl Clin Med Phys 2006;7:97-104.

7. Mechalakos JG, Hunt MA, Lee NY, Hong LX, Ling CC, Amols HI. Using an onboard kilovoltage imager to measure setup deviation in intensity-modulated radiation therapy for head-and-neck patients. J Appl Clin Med Phys 2007;8:2439.
8. Pehlivan B, Pichenot C, Castaing M, Auperin A, Lefkopoulos D, Arriagada R, et al. Interfractional set-up errors evaluation by daily electronic portal imaging of IMRT in head and neck cancer patients. Acta Oncol 2009;48:440-5.

THE ASEAN JOURNAL OF RADIOLOGY 2010: 16(2): 108-116

Original Article

Successful Diagnostic and Complication Rate in CT Guided Lung Biopsy: Comparison of Core Needle Biopsy and Fine Needle Aspiration Biopsy in Different Size Pulmonary lesions

Tanapong Panpikoon, MD., Jesada Suvikrom, MD., Prathana Mitrakul, MD., Tharintorn Treesit, MD.

Division of Interventional Radiology, Department of Diagnostic Radiology, Faculty of Medicine, Ramathibodi Hospital, Bangkok

Abstract

Objective: The aim of the study was to compare successful diagnostic and complication rate of core needle biopsy (CNB) with those of fine needle aspiration biopsy (FNAB) performed on pulmonary lesions of different sizes.

Materials and Methods: We retrospectively reviewed results and complications of 156 consecutive percutaneous CT guided biopsy of pulmonary lesions obtaining in January 2007 to July 2009, performed with either CNB (Semiautomatic cutting biopsy device 18 G) or FNAB (Spinal needle 20 G). The patients who performed with both CNB and FNAB were excluded. Fifty-four Core needle biopsies and 102 Fine needle aspiration biopsies were recorded. The successful diagnostic and complication rates of each method were compared in lesion less than 1 cm, equal 1 cm to less than 3 cm and greater than 3 cm in AP diameter.

Results: The overall successful diagnostic rate of our procedure was 76.3%. There was no statistically significant difference ($p<.05$) between successful diagnostic rate of CNB and FNAB in every size of pulmonary lesion (40.0% Vs 54.5% in lesion less than 1 cm, 78.6% Vs 69.7% in lesion equal 1 cm to less than 3 cm, 90.5% Vs 88.0% in lesion greater than 3 cm) as well as complication rate of CNB and FNAB in every size of pulmonary lesion (40% vs 36.4% in lesion less than 1 cm, 35.7%Vs28.8% in lesion equal 1 cm to less than 3 cm, 24.0% Vs 39.1% in lesion greater than 3 cm). But, there was statistically significant difference ($p<.05$) between successful diagnostic rate of lesion less than 1 cm (54.5%) and lesion greater than 3 cm (88.0%) when biopsy was performed by FNAB.

between successful diagnostic rate of lesion less than 1 cm (40.0%), lesion equal to 1 cm to less than 3 cm (78.6%) and lesion greater than 3 cm (90.5%) when biopsy was performed by CNB. There was no statistically significant difference ($p<.05$) between complication rate in every size of lesion when biopsy was performed by either CNB or FNAB.

Summary: CT guide lung biopsy is significantly less accurate for small pulmonary lesion (less than 1 cm in AP diameter) than for larger pulmonary lesion. There was no significant difference of successful diagnostic and complication rate when CT guide lung biopsy was performed by either CNB or FNAB.

Introduction

Percutaneous transthoracic needle biopsy (TTNB) using image guidance is a relatively safe and accurate method of establishing the diagnosis of pulmonary nodules, reported diagnostic accuracy for TTNB for pulmonary nodules range from 64-97%[1-5]. Computed tomography (CT) is the preferred image guidance modality for TTNB. The advantage of CT-guided lung biopsy is that the lung parenchyma and not inflated areas at the puncture site is visualized and can be used as an access path to the lesion, substantially reducing risk of pneumothorax. Such core needle biopsy (CNB) or fine needle aspiration biopsy (FNAB) is well-established method for TTNB.

FNAB is method to obtain an aspirate with a thin needle (20G or greater) which usually provides enough material to confirm or rule out malignancy by cytological analysis. In most cases, a histological diagnosis is not possible owing to an insufficient amount of material. CNB using large gauge semi-automated needle biopsy (14-19G) is a traditionally performed in patients without a known primary tumor, in cases of potential lymphoma and after inconclusive FNAB. Comparing FNAB and CNB, the latter led to a significant higher rate of specific diagnosis with same complication rate[6-7].

At our institution CT guide lung biopsy is routinely performed in most of many different lung lesions. However, we have no standard practical guideline for appropriate technique for different lung lesions. Therefore, we are interested in studying our CT guide lung biopsy experiences by compare successful diagnostic and complication rate of CNB with those of FNAB performed on different sizes of pulmonary lesions. From the result, we expected information that such CNB or FNAB is appropriate technique for either sizes of pulmonary lesion.

Materials and Methods

We retrospectively reviewed results and complications of 156 consecutive percutaneous CT guided biopsy of pulmonary lesions obtaining in January 2007 to July 2009, performed by either CNB or FNAB. The patients who performed with both CNB and FNAB were excluded. Fifty-four Core needle biopsies and 102 Fine needle aspiration biopsies were recorded.

All procedures were performed on a 16 slices multidetector CT scan. We measure long axis of pulmonary lesions on lung window settings. The lesion less than or equal 3 cm in diameter were performed on image obtained with a slice thickness of 2 mm. The lesion greater than 3 cm in diameter were performed on image obtained with a slice thickness of 2 or 5 mm. Biopsies were performed by body intervention fellowships under supervision of experience body intervention staff. Before each procedure, informed consent was obtained. Patients were placed in a supine, prone or lateral decubitus position depending on the location of the lesion. Localization was performed by CT imaging with laser light and grid system. Local anesthesia with 1% lidocaine was administered subcutaneously. Before tissue cutting or aspiration was obtained, a CT image was obtained to document successful placement of needle within the lesion.

CNBs were performed by semiautomatic cutting biopsy device 18 G with a spring activated Tru-Cut system. The tru-Cut biopsy needle is characterized by a trough at the distal end. First the biopsy gun fires inner needle into the lesion, where a core of tissue falls into the trough. Then the outer needle cuts the sample lying in the trough out of the surrounding tissue and captures the sample, which can be safely removed through the outer needle or with the whole system. Usually at least two samples were taken for histological evaluation and were instantly put into 10% formalin. FNABs were performed by spinal needle 20 G. The aspirated volume ranged between 3 and 5 ml for most aspiration biopsies, the needle was moved back and forth within the lesion for 10-15 seconds or until the hub of the syringe become filled with blood. Before the needle was removed from the lesion, the suction was stopped to avoid aspiration of further tissue potentially confusing cystologic evaluation. The specimens obtained were placed on sterile glass slides and immediately smeared. No cytopathologist or cytotechnologist was present at all biopsies.

After removal of the biopsy needle, whole CT scans of chest was performed for recognized presence of pneumothorax and then patients were immediately placed in a puncture side down position and transferred to observation ward. Talking and coughing were discouraged. We obtained chest radiographs 1 and 4 hr after biopsy. Patients with pneumothorax were administered oxygen nasal canula to speed resorption of pneumothorax. Patients with enlarging pneumothorax on serial chest radiographs and those with symptomatic pneumothorax were treated with placement of chest drainage tube.

Cytopathological results of every biopsy were recorded and classified in conclusive (positive for malignancy, suspicious for malignancy and diagnostic of specific benign entity) and non-conclusive (inadequate specimen or normal lung tissue) group. The successful diagnostic and complication rates of each biopsy were calculated and compared between 3 groups of lesion. We divided pulmonary lesion into 3 groups according to their sizes, less than 1 cm, equal 1 cm to less than 3 cm and greater than 3 cm in AP diameter, respectively. The chi-square test was used to assess the statistical significance of our results.

Results

One hundred and fifty-six CT guide lung biopsies were included in our study. 119 conclusive cytopathological results from all 156 biopsies were noted. The overall successful diagnostic rate of our

procedure was 76.3%. We have got 43 conclusive results from 54 core needle biopsies and 76 conclusive results from 102 Fine needle aspiration biopsies. The successful diagnostic rates of CNB and FNAB are about 79.6% and 77.5 %, respectively (table 1).

In group of lesion less than 1 cm, there are 16 patients in this group. We have got 2 conclusive results from 5 core needle biopsies and 6 conclusive results from 11 fine needle aspiration biopsies. The successful diagnostic rates of CNB and FNAB are about 40.0% and 54.5 %, respectively.

In group of lesion equal 1 cm to less than 3 cm, there are 94 patients in this group. We have got 22 conclusive results from 28 core needle biopsies and 46 conclusive results from 66 fine needle aspiration biopsies. The successful diagnostic rates of CNB and FNAB are about 78.6% and 69.7%, respectively.

And in group of lesion greater than 3 cm, there are 46 patients in this group. We have got 19 conclusive results from 21 core needle biopsies and 22 conclusive results from 25 fine needle aspiration biopsies. The successful diagnostic rates of CNB and FNAB are about 90.5% and 88.0%, respectively.

FNAB shows slightly higher successful diagnostic rate in lesion less than 1 cm where as CNB shows slightly higher successful diagnostic rate in lesion equal to greater than 1 cm. However, there is no statistically significant difference ($p<.05$) between successful diagnostic rate of CNB and FNAB in any size of pulmonary lesion (table 2).

When we compared the successful diagnostic rate between the groups of different in size of lesion, there are statistically significant difference ($p<.05$) between successful diagnostic rate of lesion less than 1 cm (54.5%) and lesion greater than 3 cm (88.0%) when biopsy was performed by FNAB, between diagnostic accuracy of lesion less than 1 cm (40.0%), lesion equal to 1 cm to less than 3 cm (78.6%) and lesion greater than 3 cm (90.5%) when biopsy was performed by CNB.

The major complication we concerned after CT guide lung biopsy is pneumothorax. 50 patients (32.0%) develop pneumothorax after procedure, 21 patients from CNB group and 29 patients from the FNAB group. Only 2 patients from CNB group (1.3%) have enlarging pneumothorax on serial chest radiographs and symptomatic pneumothorax after CNB. They were treated with placement of chest drainage tube.

Table 1 Conclusive cytopathological result, successful rate and complication(pneumothorax) rate of CNB and FNAB from CT guide lung biopsy

	CNB	FNAB	CNB+FNAB
Conclusive cytopathological result	43	76	119
Inconclusive cytopathological result	11	26	37
Pneumothorax	21	29	50
Total	54	102	156
Successful diagnostic rate	*79.6%*	*74.5%*	*76.3%*
Complication rate (pneumothorax)	*38.9%*	*28.4%*	*32.0%*

In group of lesion less than 1 cm, there are 16 patients in this group. Two of 5 patients from CNB groups and 4 of 11 patients from FNAB group have pneumothorax. The complication rates of CNB and FNAB are about 40.0% and 36.4%, respectively.

In group of lesion equal 1 cm to less than 3 cm, there are 94 patients in this group. Ten of 28 patients from CNB groups and 19 of 66 patients from FNAB group have pneumothorax. The complication rates of CNB and FNAB are about 35.7% and 28.8%, respectively.

And in group of lesion greater than 3 cm, there are 46 patients in this group. Six of 21 patients from CNB groups and 9 of 25 patients from FNAB group have pneumothorax. The complication rates of CNB and FNAB are about 28.5% and 36.0%, respectively. Using Chi-square test, there was no statistically significant difference ($p<.05$) between complication rate in every size of lesion when biopsy was performed by either CNB or FNAB. (Table 3).

Discussion

Percutaneous transthoracic needle biopsy (TTNB) using CT guidance is a relatively safe and accurate method of establishing the diagnosis of benign and malignant pulmonary lesion. With the recommended co-axial technique, reported diagnostic accuracy for TTNB for pulmonary nodules range from 64-97% and major complications are rare[1-5]. Pneumothorax is the most common complication after procedure with reported rate of 19-44%[8], the range of reported rates of ICD insertion is 1.6-4.3%.

Due to our retrospective comparative study

Table 2 Comparison of successful diagnostic rate between CNB and FNAB in different size of lesion

Size of lesion	CNB		FNAB		Statistical difference by Chi-square test ($p<0.05$)
	Conclusive result /All	Successful diagnostic rate	Conclusive result/All	Successful diagnostic rate	
less than 1 cm	2/5	*40.0%*	6/11	*54.5%*	No
equal 1 cm to less than 3 cm	22/18	*78.6%*	46/66	*69.7%*	No
greater than 3 cm	19/21	*90.5%*	22/25	*88.0%*	No

Table 3 Comparison of complication rate between CNB and FNAB in different size of lesion

Size of lesion	CNB		FNAB		Statistical difference by Chi-square test ($p<0.05$)
	Pneumothorax	Complication rate	Pneumo-thorax	Complication rate	
less than 1 cm	2/5	40.0%	4/11	36.4%	No
equal 1 cm to less than 3 cm	10/28	35.7%	19/66	28.8%	No
greater than 3 cm	6/21	28.6%	9/25	36.0%	No

design, we have some important limitation. First, we cannot compare diagnostic accuracy rate of both technique. So, we use the term "successful diagnostic rate" instead of diagnostic accuracy rate. Many influencing factor for pneumothorax or other complication risk were not recorded. However, we got many interesting information from our study.

Our results show that 76.3 % of successful diagnostic, 32.0% complication rate and 1.3% of ICD insertion rate from our experience are in the average range from worldwide reports. Even through, we not routinely use recommended co-axial technique. No statistical significant difference of successful diagnostic and complication rate between CNB and FNAB were founded on every different size of pulmonary lesions. From this information, we do not worried about different efficacy of both technique and should routinely done TTNB by CNB or FNAB technique according to standard recommended guideline. FNAB is suitable for tissue sampling of pulmonary lesion given a known primary tumor in combination with suspected metastases. It is generally considered insufficient if the primary tumor is unknown. CNB or large-gauge

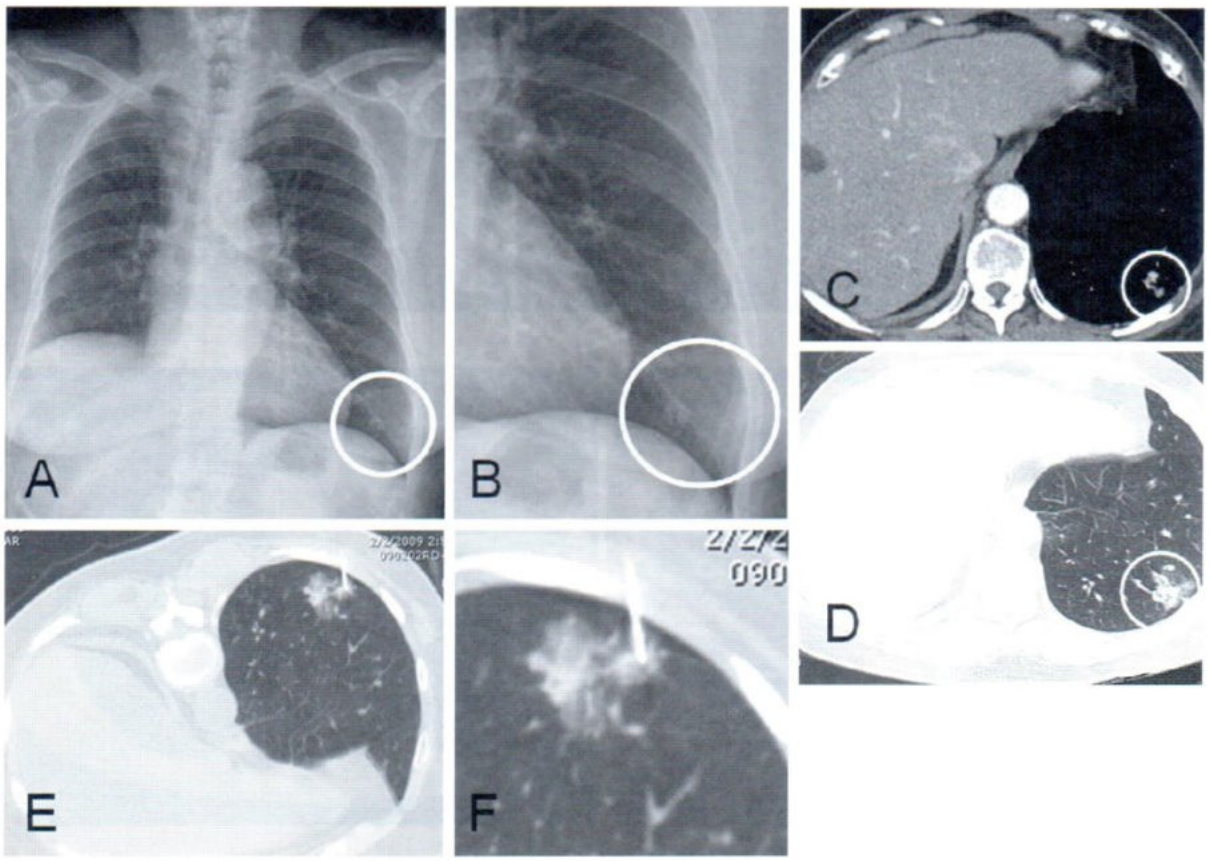

Fig.1 A 73 years old woman presented with abnormal chest film. Her chest film showed nodular opacities at left lower lung field (A, B). After that CT scans of chest was done and showed group of nodular opacities with surrounding ground glass opacity (C, D). Percutaneous transthoracic FNA biopsy was performed by using spinal needle No.20G (E, F) and cytological report showed positive for malignant cells. Then, she undergone pneumonectomy and pathological result shows adrenocarcinoma.

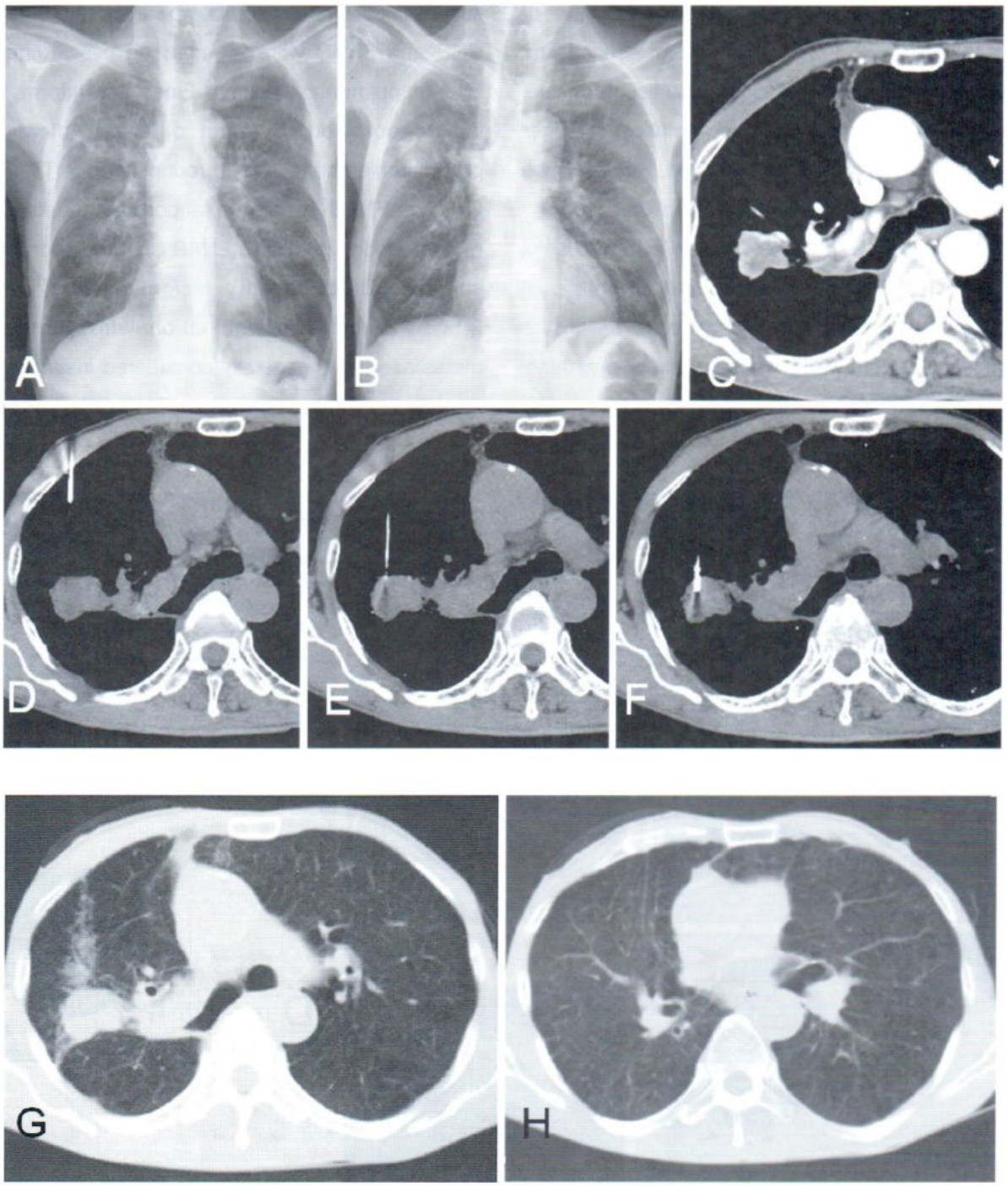

Fig.2 A 70 years old man presented with developing of RUL mass from May 2008 (A) to February 2009 (B). CT scans of chest was done and showed enhancing mass at RUL. Percutaneous transthoracic Core needle biopsy was performed by using Semi automatic cutting devices No.18 G X I attempt (D, E, F) and pathological report showed brochoalveolar carcinoma (BAC). CT scans of chest after TTNB (G, H) showed pulmonary hemorrhage along the needle tract. No pneumothorax was observed.

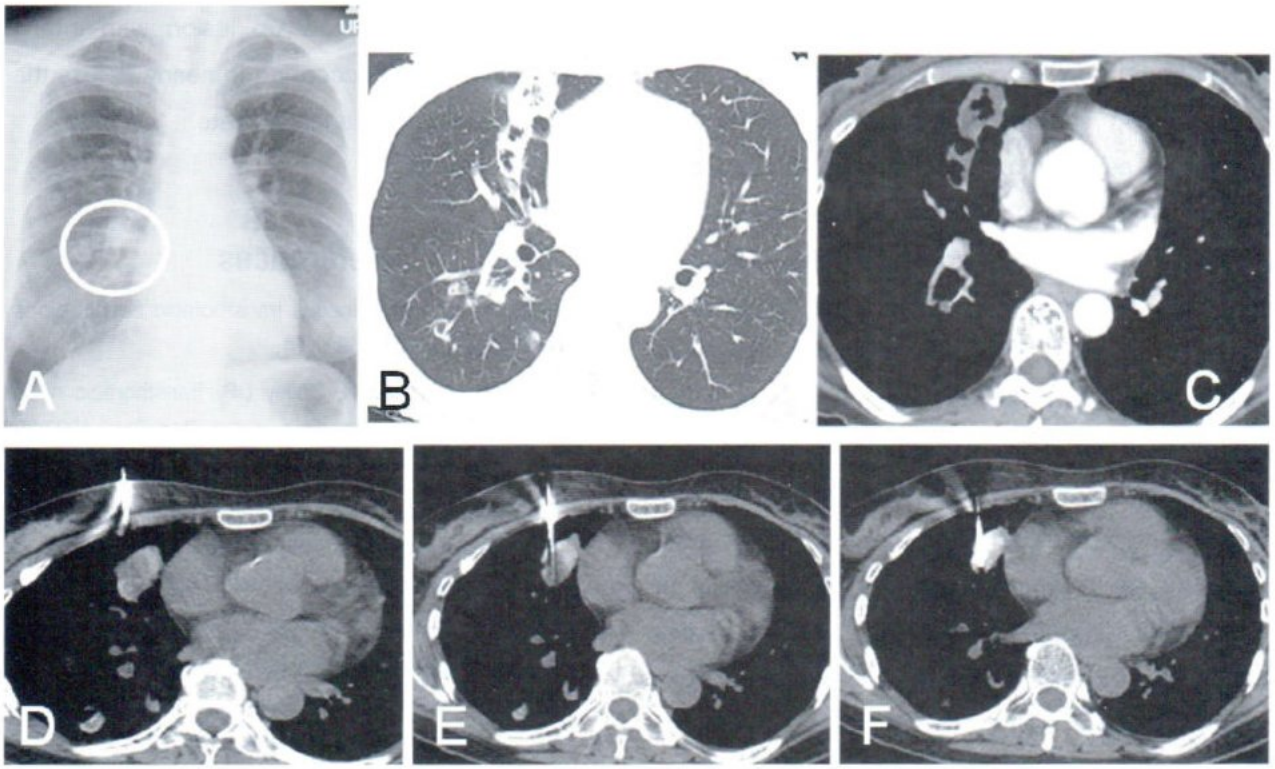

Fig.3 A 48 years old woman known case of Rheumatoid arthritis presented with multiple pulmonary masses (A). CT scans of chest was done and showed multiple pulmonary nodules and some of them have cavitary formation (B, C). Percutaneous transthoracic Core needle biopsy was performed by using Semi automatic cutting devices No.18 G X I attempt (D, E, F) at the RML mass and pathological report showed Cryptococcosis.

automated needle biopsy is traditionally performed in patients without a known primary tumor, in cases of potential lymphoma and after inconclusive FNAB. Owing to the varying availability of a cytopathologist and results that are comparable to those of FNAB (or even better), CNB has meanwhile been established as the primary technique of choice.

Previous studies have reported accuracies for TTNB of small and large size of pulmonary lesion that conflict with on another[9,10,11]. Although the criteria for small nodules are arbitrary, we defined such nodules as being less than 1 cm in diameter. Our rationale for this size criterion is that in our experience, on the basis of size alone, lesion greater than 1 cm in diameter usually do not pose technical difficulty, where as small nodules often are technically challenging. From our study, there are statistically significant difference ($p<.05$) between successful diagnostic rate of lesion less than 1 cm (54.5%) and lesion greater than 3 cm (88.0%) when biopsy was performed by FNAB, between successful diagnostic rate of lesion less than 1 cm (40.0%), lesion equal to 1 cm to less than 3 cm (78.6%) and lesion greater than 3 cm (90.5%) when biopsy was performed by CNB. This information confirmed that pulmonary lesions less than 1 cm in diameter pose technical difficulty and cause less successful diagnostic rate with either CNB or FNAB. We may

ask pulmonologist for close follow up lesion with interval imaging than TTNB according to nearly or less than 50% of successful diagnostic rate.

Varying complication rate of different size pulmonary lesions in both CNB and FNAB are shown in our study. The small lesions (less than 1 cm) show slightly higher complication (pneumothorax) rate than the large lesion (larger than 3 cm), likely to be from more technical difficulty and more number of pleural pass. However, other many factor that may effect risk of pneumothorax such as number of pleural pass, distance of pleural surface, location of pulmonary lesion, presence of emphysema/degree of emphysema and training level of fellow who done TTNB were not included in this study. With this information, we interested and have planning for our next study with purpose of study for examine multiple variable factor that effect risk of pneumothorax after TTNB.

Conclusion

Percutaneous transthoracic needle biopsy (TTNB) using CT guidance is a relatively safe and accurate method of establishing the diagnosis of benign and malignant pulmonary lesion. There is no difference between successful diagnostic and complication rate of CNB and FNAB. FNAB is suitable for tissue sampling of pulmonary lesion given a known primary tumor in combination with suspected metastases. CNB or large-gauge automated needle biopsy is traditionally performed in patients without a known primary tumor, in cases of potential lymphoma and after inconclusive FNAB.

The pulmonary lesions less than 1 cm in diameter pose technical difficulty, cause less successful diagnostic rate and more complication rate with either CNB or FNAB. We may ask pulmonologist for close follow up lesion with interval imaging than TTNB according to nearly or less than 50% of successful diagnostic rate.

References

1. Westcott JL. Percutaneous transthoracic needle biopsy: Radiology 1988;169:593-601.
2. Westcott UJL, Rao N, Colley DP. Transthoracic needle biopsy of small pulmonary nodules. Radiology 1997;202: 97-103.
3. Swischuk JL, Castaneda F, Petal JC, et al. Percutaneous transthoracic needle biopsy of the lung: review of 612 lesions. J Vasc Interv Radiol 1998;9:347-52.
4. Laurent F, Latrable V, Vergier B, et al. CT-guided transthoracic needle biopsy of pulmonary nodules smaller then 20 mm: results with an automated 20-gauge coaxial cutting needle. Clin Radiol 2000;55:281-7.
5. Tsukada H, Satou T, Iwashima A, et al. Diagnostic accuracy of CT guided automated needle biopsy of lung nodules. AJR Am J Roentenol 2000;175:239-43.
6. Anderson JM et al. CT-guided lung biopsy: factors influencing diagnostic yield and complication rate. Clin Radiol 2003;58(10):791-7.
7. Charig MJ, Phillips AJ. CT-guided cutting needle biopsy of lung lesions-safety and efficacy of an out-patient service. Clin Radiol 2000;55(12):964-9.
8. Shepard JO. Complications of percutaneous needle aspiration biopsy of the chest; prevention and management. Semin Intervent Radiol 1994;11:181-5.
9. VanSonnenberg E, Casola G, Ho M, et al. Difficult thoracic lesions: CT guided biopsy experience in 150 cases. Radiology 1988;167:457-61.
10. Poe RH, Tobin RE. Sensitivity and specificity of needle biopsy in lung malignancy. Am Rev Respir Dis 1980;122: 725-9.
11. Hayata Y, Oho K, Ichiba M, et al. Percutaneous puncture for cytologic diagnosis:its diagnostic value for small peripheral pulmonary carcinoma. Acta Cytol 1973;17: 469-75.

THE ASEAN JOURNAL OF RADIOLOGY 2010; 16(2): 117-121 117

Original Article

Evaluation of the Setup Error using On-Board Imager (OBI) System in Upper Abdominal Cancer

Natchayaporn Thonapan, B.Sc., Wilai Masa-Nga, B.Sc., Sawanee Suntiwong, B.Sc., Kittipol Dachaworakol, B.Sc., Sangutid Thongsawat, M.Sc., Chirasak Khamfongkhruea, B.Sc., Chirapha Tannanonta, M.Sc.

Department of Radiation Oncology Unit, Chulabhorn Hospital, Bangkok, Thailand

Abstract

Purpose: To study the setup error of patient's positioning in upper abdominal cancer.

Materials and Methods: Eleven patients with upper abdominal cancer treated by 3D-CRT and IMRT techniques were studied during June 2008 to February 2009. Pre-treatment process began when two images in AP and Lat views of the patient were captured by using the OBI (Onboard Imager) System that attached with the linear accelerator machine. These two images were overlaid with the reference DRR (Digital reconstruction radiograph) of the planning CT (in the same views). As a consequence, the setup or couch position errors compared with the treatment planning values in three directions were calculated by the OBI software. Once the shifts applied, the couch had automatically moved to the right positions before treating the patient.

Results: For 134 OBI sessions, the average errors were 0.18±0.14 cm (0 - 0.7 cm), 0.24±0.22 cm (0-1.0 cm) and 0.21±0.18 cm (0 - 0.7 cm) in vertical (Vrt), longitudinal (Lng) and lateral (Lat) directions respectively. The maximum setup error was 1.0 cm in the Lng direction for a single patient. However, the errors within 0.5 cm in these three directions resulted as 99%, 88%, and 93%.

Conclusion: Most of the setup error values were acceptable within 0.5 cm in the entire directions; Vrt, Lng and Lat. Using OBI system, the patients were typically treated in the same position as mentioned in the treatment planning that helps to increase tumor control probability and decreasing complication rate.

Introduction

In radiation therapy, patient's positioning and immobilization referred as a concerning process since the error of these processes may result in tumor control and patient complication. The optimization in radiotherapy functioned to deliver maximum dose to the tumor and minimum dose to the normal tissue. One method that increases efficiency according to the goal of radiotherapy would recognize ultimately on declining the setup error of patient's positioning and immobilization processes[1-3]. Therefore, it could be strongly supporting that the study of setup error from patient's positioning and immobilization was a crucial consideration. Numerous verification devices were implemented to check the patient's position before treatment such as port film[4,5], electronic portal imaging device (EPID)[6] and on-board imager (OBI)[7]. It was decided particularly for this case that, the patient's position was checked by using a kV OBI from Varian Medical Systems (Palo Alto, CA, USA). We selected this device as a result of, its high quality image, reducing radiation dose, having automated matching software and capability of shifting the couch automatically to the accurate position.

Fox et al[8] studied the performance of image registration software and repositioning 3D offset using OBI software. They tested precision and accuracy in known offset phantom (geometric rigid phantom and anthropomorphic head phantom). The accuracy of the OBI in detecting the positioning was represented with less than 1.4 mm for 3D vector offset (0.8 mm, 1.1 mm, and 0.4 mm in Vrt, Lng, and Lat directions respectively).

Perkins et al[9] analyzed the setup errors of thirteen patients with primary gastrointestinal cancer by using a kV OBI. The errors in three directions (Vrt, Lng, and Lat) were recorded with the average values of 0.32±0.42 cm (Vrt), 0.33±0.34 cm (Lng), and 0.35±0.39 cm (Lat). The percentage errors with equal to or less than 0.5 cm were 25% (Vrt), 28% (Lng), and 30% (Lat). They reported that by using OBI kV-kV matching, the uncertainty was reduced in amount of dose delivered, potentially resulting in improvement in local control and reduction in treatment toxicity.

This study was designed to evaluate the setup errors of the patient positioning for upper abdominal cancer in Radiation Oncology Unit, Chulabhorn Hospital.

Materials and Methods

This study was retrospective of 134 sessions from 11 patients with upper abdominal cancer during June 2008 to February 2009.

Before starting to treat each patient, two images, AP (antero-posterior) and lateral were taken by utilizing the kV OBI attaching with the treatment machine of Varian Medical Systems (Palo Alto, CA, USA). These images were compared with the DRR (Digital Reconstructed Radiograph) generating from the planning CT images by using kV-kV matching software of the OBI as shown in Fig.1. The automatically matching of the images was performed first, however, if it was not proper matched, the manual matching with bony landmarks would be done by a radiation oncologist (in the first fraction). After the matching was accepted, the setup errors or couch shifting values in three directions, Vrt, Lng and Lat were determined by the software and the couch substantially moved into the correct positions after the shift was applied.

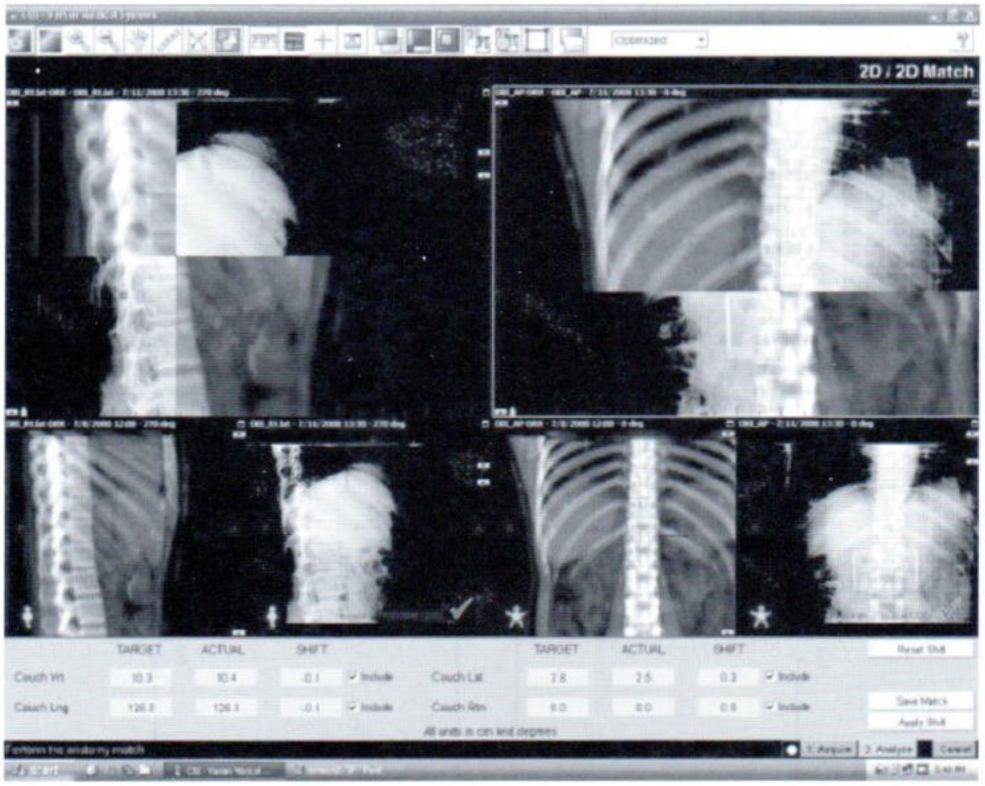

Fig.1 The OBI console shows the overlaid images of OBI and reference images and couch shift (error) values

Results

Table 1 shows the maximum, minimum and average values of the errors in the three directions for 134 OBI sessions of 11 patients. The maximum error was 1.0 cm in Vrt direction with the mean of 0.24±0.22 cm.

The frequency and percentage of errors in various ranges were summarized and shown in Table 2. The Vrt, Lng and Lat directions present the errors within 0.5 cm. with 99%, 88% and 93% respectively.

Fig.2 shows the scatter plots of the setup errors of each session in AP and Lat views. The errors of Lat direction shown in Fig.2(a) were almost in the positive (left) side of the patient which may affect from the systematic error.

Table 1 Setup error of patient positioning for upper abdomen

Vrt		Lng		Lat	
Mean±SD	**Min - Max**	**Mean±SD**	**Min - Max**	**Mean±SD**	**Min - Max**
0.18±0.14	0 - 0.7	0.24±0.22	0 - 1.0	0.21±0.18	0 - 0.7

Table 2 Frequency of setup errors in number of fractions and percentage in the three directions for various ranges of upper abdominal patients

Error (cm)	Vrt	Lng	Lat
0 - 0.1	71 *(53%)*	58 *(43%)*	59 *(44%)*
0.2 - 0.3	44 *(33%)*	44 *(33%)*	47 *(36%)*
0.4 - 0.5	18 *(13%)*	17 *(12%)*	18 *(13%)*
0.6 - 0.7	1 (1%)	13 (10%)	10 (7%)
0.8 - 0.9	0 (0%)	1 (1%)	0 (0%)
1.0 - 1.1	0 (0%)	1 (1%)	0 (0%)
Total	134 (100%)	134 (100%)	134 (100%)

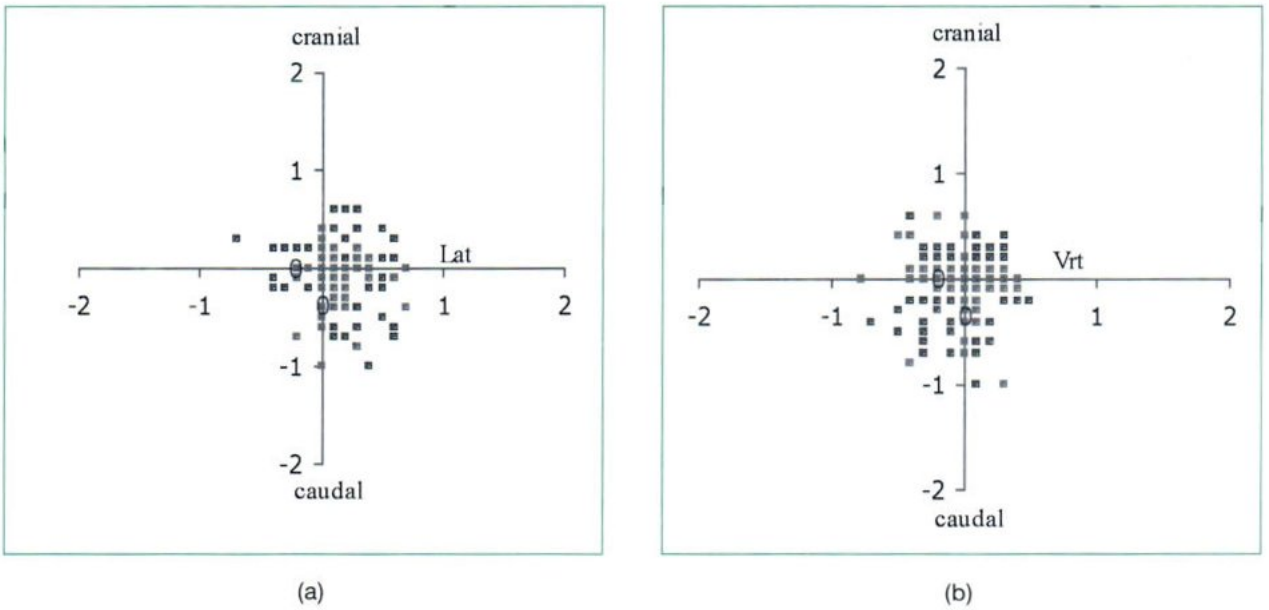

Fig. 2 The scatter plots of setup error values: (a) AP and (b) lateral views of the images (Each point represents each session)

Discussion

Our study showed a comparable result with the one of Perkins et al1 with the ratio, Perkins / this study as: (0.30±0.42) / (0.18±0.14), (0.33±0.34) / (0.24±0.22) and (0.35±0.39) / (0.21±0.22) in Vrt, Lng and Lat directions respectively.

For each patient, the majority errors were mostly appeared in the same sign of the co-ordinate for all directions with every session, hence these can be caused by the plan transferring error and the difference of the patient positioning on CT and treatment tables. When the error came out

apparently more than 0.5 cm, the condition of the patient had to be carefully considered and noted.

From the error values shown after image matching, the treatment couch can be automatically shifted to the right positions in the three directions before the treatment starts. The OBI is useful in external beam treatment as the patient was treated in the same position to the one used in the planning system. It results as high tumor control probability and low complication rate.

Conclusion

Most setup error values of the three directions (Vrt, Lng, Lat) were measured within 0.5 cm. Only a single patient with fatty abdomen represented the error of 1.0 cm in the Lng direction for 2 sessions. A Vac-Lok may help to decrease the error of this patient but it could increase positioning setup time.

Whether institute where the OBI is not available, the larger PTV still be considerable. The OBI will be notified, when the tumor is close to a critical organ. Anyhow, if an internal organ movement from respiration takes place, more advance modality, respiratory gating is the concerning factor[10-12].

The comparison of positioning errors of the patient with and without Vac-Lok will be on-going for the further study[13].

References

1. Phllips MH, Singer K, Miller E, Stelzer K. Commissioning an image-guided localization system for radiotherapy. Int J Radiat Oncol Biol Phys 2000;48:267-76.
2. Marks JE, Haus AG. The effect of immobilization on localization error in the radiotherapy of head and neck cancer. Clinical Radiology 1976;27:175-7.
3. Goitein M, Busse J. Immobilization error: some theoretical considerations. Radiology 1975;117:407-12.
4. Hurkmans CW, Remeijer P, Lebesque JV, Mijnheer BJ. Set-up verification using portal imaging: review of current clinical practice. Radiotherapy Oncology. 2001; 58:105-20.
5. Bel A, Van Herk M, Bartilink H, Lebesque JV. A verification procedure to improve patient set-up accuracy using portal images. Radiotherapy Oncology. 1993;29:253-60.
6. Chyty K, McCurdy BM. Comprehensive fluence model for absolute portal dose image prediction. Med Phys 2009;36:1389-98.
7. Hong LX, Chen CC, Garg M, Yaparpalvi R, Mah D. Clinical experiences with onboard imager KV images for inear accelerator-based stereotactic radiosurgery and radiotherapy setup. Int J Radiat Oncol Biol Phys 2009;73: 556-61.
8. Fox T, Huntzinger C, Johntone P, et al. Performance evaluation of an automated image registration algorithm using an integrated kilovoltage imaging and guidance system. Applied Clinical Medical Physics 2006;7:97-104.
9. Charles LP, Fox T, Elder E, et al. Image-Guided Radiation Therapy (IGRT) in gastrointestinal tumors. Journal of the Pancreas 2006;7:372-81.
10. Kutcher GJ, Mageras GS, Liebel SA. Control, Correction, and Modeling of Setup Errors and Organ Motion. Seminars in Radiation Oncology 1995;5:134-45.
11. Mah D, Hanley J, Rosenzweig KE, et al. Technical aspects of the deep inspiration breath-hold technique in the treatment of thoracic cancer. Int J Radiat Oncol Biol Phys 2000;48:1175-85.
12. Wong JW, Sharpe MB, Jaffray DA, et al. The use of active breathing control (ABC) to reduce margin for breathing motion. Int J Radiat Oncol Biol Phys 1999;44: 911-9.
13. Malone S, Szanto J, Perry G, et al. A perspective comparison of three systems of patient Immobilization for prostate radiotherapy. Int J Radiat Oncol Biol Phys 2000;48:657-65.

THE ASEAN JOURNAL OF RADIOLOGY 2010; 16(2): 122-129

Original Article

Accuracy Verification of the Plan Evaluation Tools on Eclipse Treatment Planning System Version 8.1

Lalida Tuntipumiamorn, M.Sc.[1], Lukkana Apipunyasopon, M.Sc.[1], Porntip Lampongpaiboon, M.Sc.[1], Nuanpen Damrongkijudom, Ph.D.[2], Piyanan Liammookda, M.Sc.[1]

[1] *Division of Radiation Oncology, Department of Radiology, Faculty of Medicine, Siriraj Hospital, Mahidol University, Bangkok 10700, THAILAND*

[2] *Department of Radiological Technology , Faculty of Medical Technology, Mahidol University, Bangkok 10700, THAILAND*

Abstract

Objectives: Performance of the dose display and cumulative dose volume histogram(DVH) tools on Eclipse version 8.1 treatment planning system (TPS), was investigated using IAEA TRS-430 test protocol.

Materials & Methods: All tests were carried out by using a simple plan on a water-like test phantom. The agreement of isodose lines with color wash and point doses, reports of the hot spot and cold spot dose, correct representation of relative and absolute dose on plan normalization and consistency of dose display with varied total dose were evaluated. For cumulative DVH, some basic parameters for DVH calculations such as volume of structure, dimension of histogram dose bin and calculation grid were investigated. Relative or absolute mode DVH, DVH dose statistics and DVH statistical reports were all the subjects of interest for assessment the cumulative DVH characteristics.

Results: Consistency of the dose display tool was well maintained, since most of the deviations on all tests were found to be within ± 2 mm. For cumulative DVH, discrepancies of the calculated volumes, ranging in size from < 1 cc (optic chiasm) to > 10,000 cc (body) were shown to be within ± 2 % of the known volumes. The reported doses and volumes on DVH statistical reports and graphs were exhibited accurately. Dose statistics were correctly presented. Varying histogram dose bin from 1 cGy to 5 and 10 cGy, showed the variations in DVH calculations about 2% and 5%, respectively. In the present work, size of the calculation grid showed no effect on DVH calculations. Relative or absolute mode DVH were also found to effectively perform.

Discussion & Conclusion: General performance of the Eclipse 8.1 plan evaluation tool, was evaluated to be accurate for clinical implementation. For more complicated application, uncertainty in DVHs should be addressed with further investigation.

Keywords: plan evaluation, quality assurance, dose volume histogram, cumulative DVH, IAEA TRS-430

Introduction

Plan evaluations, using dose display and dose volume histogram, are found to be one of the most important tools in state-of-art in radiotherapy planning. Commonly, the standard display is the color-coded isodose lines or color wash which assigned color values corresponding to dose to each pixel on the display, paints the whole dose distribution in a transparent band of color overlaid on the grey scale 2D images. To perform plan optimization, dose verification and quality assurance testing, display as a "point dose" is additionally needed.[1] For analysis of treatment planning dose distributions, plan comparisons by dose volume histogram (DVH), which display how much of the volume of each structure receives how much dose, are also shown to be an efficient tool.[2-4] Currently, not only used for the plan evaluation, dose volume histogram is also being used as input data (DVH constraints) for intensity modulated radiation therapy (IMRT) planning. Hence, accuracy of the DVH performance should be verified.[5-7] In this study, investigation of the characteristics of dose display and cumulative DVH tools on Eclipse version 8.1 TPS was carried out through a series of test as recommended in the IAEA Technical Report Series no. 430 (TRS-430).[5]

Materials & Methods

A simple plan using a single field, 10 MV photon, 10x10 cm^2 with 100 cm SSD on a virtual water-like phantom (2 mm slice thickness, 30x30x30 cm^3 in size) with a prescribed dose 2 Gy at depth of 10 cm, was generated on Eclipse 8.1 TPS. Dose distribution was calculated using triple A algorithm and displayed as the isodose lines in all three axes; axial, sagittal and coronal plane. To determine an agreement of the isodose lines with the color wash and point doses, points were marked at the selected isodose level. Distances between the mark points and central axis beam were then measured and compared. In the experiments, isodose levels in the axial and sagittal plane from 150% to 50% and 100% to 5% in the coronal plane (with 5% interval) were examined. Consistency of dose display when transforming plan normalization from percent to absolute dose and varying total prescription dose from 2 Gy to be 50 Gy were also included in the investigation.

For cumulative DVH, the first aspect to be tested was the accuracy of calculated volume as determined by the system. Various size and shape perspex phantoms underwent CT scanner were exported to the Eclipse 8.1 TPS. The test objects, ranging in size from < 1 cc to > 10,000 cc, were selected to represent anatomical organs such as optic chiasm , eyeball and spinal cord. The smallest one used in the study was a perspex rod only 0.5 cm in diameter and 2.5 cm long , as shown in fig.1 (a). Using the threshold HU at -350 with no post-processing, auto-body contours were performed. Optimal window level was also adjusted until all the complete contours were obtained. Volume readings by the system were then recorded and compared with the known volume of the test objects. Ability of the Boolean logic to define compound structures was also verified. Two virtual structures with known size were created and used Boolean operators; AND, OR, XOR and SUB in the Eclipse 8.1 TPS to generate the overlap structures (fig.1b). Accuracy of the DVH calculations, when histogram dose bin were varied from 1 cGy to be 5 and 10 cGy, and dimension of calculation grid from routine 2.5 mm to be 1.25 and 5 to 10 mm, were

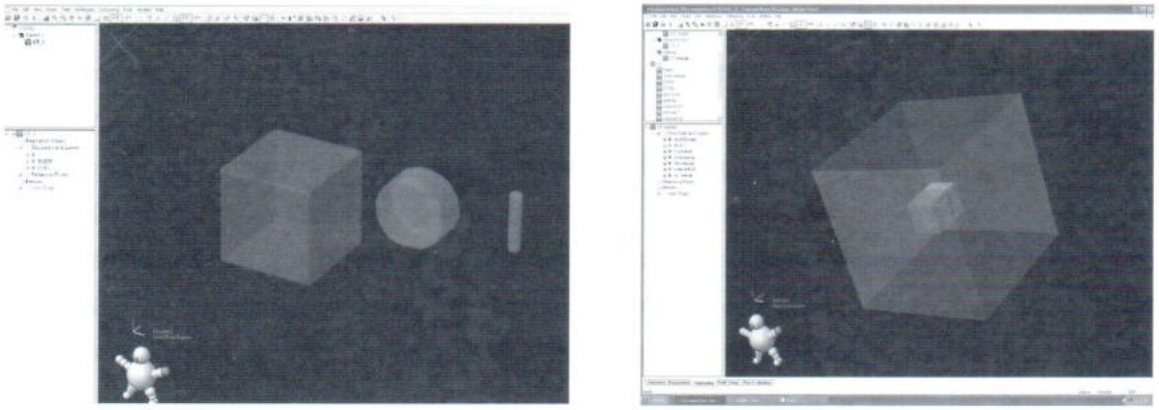

(a) (b)

Fig.1 Reconstructed volume from known dimension phantoms and compound structures using Boolean operators were generated on the Eclipse 8.1 TPS. The calculated volumes were then compared with the expected volume

studied. DVH statistical reports from two plans containing the same total dose, 2 Gy x 25 fractions and 50 Gy x 1 fraction, were exported as ASCII files. Then, agreement of the dose readings between these two plans were checked. DVHs based on either relative or absolute dose method were tested on two different plans, single-field and four-fields techniques. Report of the hot spot and cold spot dose which presented both on the isodose distribution display and dose statistics as Max dose, Min dose and Mean dose were compared with the expected values from the exported dose-volume data on ASCII files.

Results

Accuracy of the dose display tool

Consistency of the dose display tool on Eclipse 8.1 TPS was found to be acceptable. At the isodose levels from 150%-50% in the axial and sagittal plane, and from 100%-5% in the coronal plane, the majority of the deviations in all test cases were observed to be within ± 2 mm. Maximum deviation, about ± 2.8 mm, can be seen only at isodose level of 145% in the transverse plane on the test of isodose lines agreement with color wash and at 55% isodose level in the sagittal plane with relative and absolute dose test as shown in fig.2.

Cumulative Dose Volume Histograms Tool

Accuracy of the volume reading

Accuracy of Eclipse 8.1 TPS in determining the structure volumes was found to be satisfied. It is seen that, on the test objects (0.5-13824 cc), all deviations were generally about -2% (fig.3). Boolean compound volumes were also demonstrated to be accurate from - 0.03 to -3.39% (fig.4). All calculated volumes were underestimated due to the Eclipse's contouring software which smoothed the contour edge for the reconstructed volume.[15]

Effect of histogram dose bin width and calculation grid size on DVH calculations

Histogram dose bin width and calculation grid size are the main factors influencing the DVH

Fig.2 Consistency of the dose display, as isodose lines, color wash and point doses, as relative or absolute dose and when varying total doses in three axes, was found to be within ± 2 mm.

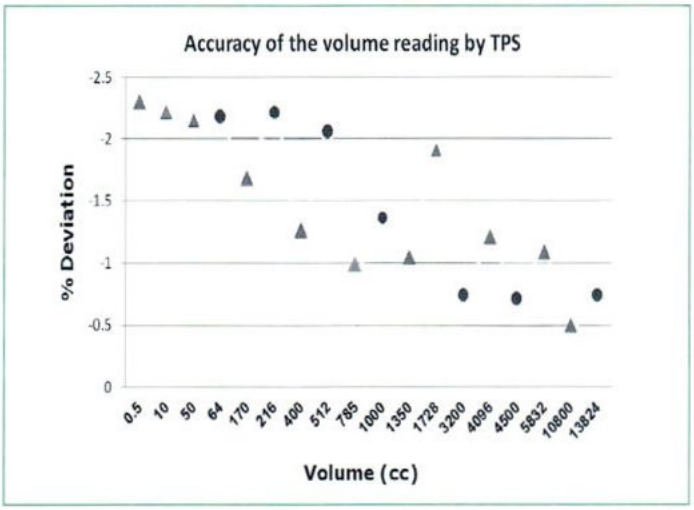

Fig.3 The percentage deviation between calculated and expected volume on Eclipse 8.1 TPS. Circle and triangle dots represent cube and cylindrical structures, respectively.

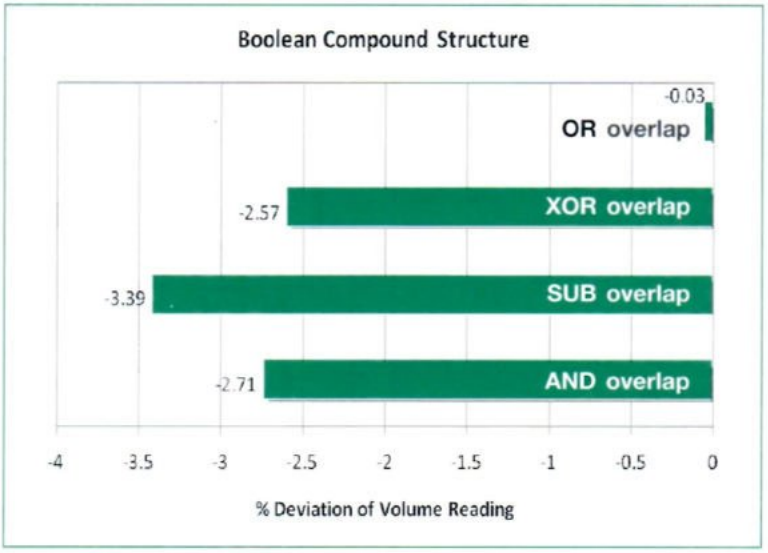

Fig.4 Uncertainty of the calculated volume found on Boolean compound structures when using AND, SUB, XOR and OR overlap operators

calculation. At the calculation grid 2.5 mm, when histogram dose bin was changed from 1 cGy to be 5 cGy, dose readings at 95%, 90% and 50% of the volume on cube and cylindrical objects were under-estimated within 2%. The variations were increased to be 3-5% when histogram dose bin was set to be 10 cGy, as shown in fig.5.

(a) Cube objects (b) Cylindrical objects

Fig.5 Variation of the dose readings on cube and cylindrical test objects when dose bin sizes at 1, 5 and 10 cGy were used for the DVH calculations

Table 1 Percent of dose difference between two plans, containing the same total dose, on cube and cylindrical objects, on the verification of the consistency of dose statistic report on cumulative DVH

Object	Volume Level	Dose Reading from DVH Statistical Report		
		2 Gy x 25	50Gyx1	% Difference
Cube	Maximum	41.75	42.04	*0.69*
	Minimum	58.25	58.1	*-0.26*
	Mean	49.5	49.6	*0.20*
Cylinder	Maximum	42.25	42.61	*0.84*
	Minimum	58.25	58.14	*-0.19*
	Mean	49.5	49.63	*0.26*

Table 2 Accuracy of the dose statistic readings when compared with the expected values on ASCII files

Object	Dose Level	Dose Readings(cGy)			% Difference from ASCII file data	
		Hot/Cold Spot	Dose Statistics	Exported Data	Hot/Cold Spot	Dose Statistics
Square	Maximum	2.32	2.32	2.33	*-0.43*	*-0.43*
	Minimum	1.69	1.69	1.69	*0.00*	*0*
	Mean	1.99	1.98	1.98	*0.51*	*0*
Cylinder	Maximum	2.32	2.32	2.33	*-0.43*	*-0.43*
	Minimum	1.71	1.68	1.69	*1.18*	*0.59*
	Mean	1.99	1.98	1.98	*0.51*	*0*

About the dimension of calculation grid, no significant difference of the cumulative DVHs computed from various calculation grids can be observed in this study. Dose readings on the DVH statistical reports were examined and all deviations on various test structures were found to be less than ±1%.

DVH statistical report and dose statistics

DVHs on two plans containing the same total dose, 2 Gy x 25 fractions and 50 Gy x 1 fraction, were exported as ASCII files and the results in Table 1 showed the consistency of DVH statistical report was within ±1%.

For dose statistics, comparison of the hot spot and cold spot dose on the isodose display and on the structure of plan (Max, Min, and Mean Dose) found them to be within 0-1.2% of the expected values from ASCII files as presented in Table 2.

DVH as relative and absolute dose mode

Relative and absolute dose DVHs on two different plans were demonstrated to perform properly. Results of the study showed the overall

Table 3 Comparisons of the dose readings from cumulative DVHs when displayed as relative and absolute dose mode on single-field and four-field technique plans

Object	Dose Level	Cumulative DVH					
		Single-field Technique			Four-field Technique		
		Relative	Absolute	% Difference	Relative	Absolute	% Difference
Cube	Maximum	2.32	2.33	*0.43*	2.01	2.03	*0.99*
	Minimum	1.68	1.67	*-0.60*	1.94	1.93	*-0.52*
	Mean	1.98	1.98	*0*	2	1.99	*-0.50*
Cylinder	Minimum	1.7	1.69	*-0.59*	1.94	1.93	*-0.52*
	Maximum	2.33	2.33	*0*	2.03	2.03	*0*
	Mean	1.98	1.98	*0*	1.99	1.99	*0*

deviations, at different dose levels, were less than 1%, as shown in Table 3.

Discussion & Conclusion

It is crucial for the overall quality of treatment that the characteristics of plan evaluation tools should be included in the assessment of a 3D treatment planning system. In our work, investigation of the accuracy of plan evaluation tools was proposed to complete the quality control process for the commercial TPS.

Many investigators had proposed the methods to evaluate the uncertainty in DVH calculations[9-13]. However, we found that the basic test protocol from IAEA Technical Report Series no. 430 was useful and convenient for our first step when examining the dose display and DVH capabilities and limitations.

To verify the accuracy of volume as determined by the Eclipse 8.1 TPS, we attempted to select test objects which closely represented the human anatomical organs. It was confirmed that, the system is able to provide an adequate accuracy of about 2%, even in the 0.5 cc rod structure which represents the optic chiasm.

Investigation of plan evaluation tools in this study was only performed by using the simple plan and homogeneous phantom. However, there was a report on quality assurance of DVHs in more complicated condition. DVHs in 9 IMRT planning from XKnife(tm) RT2 TPS, were verified with the Monte Carlo methods and the results indicated that the DVHs predicted by both methods were acceptable for the treatment execution[16].

In summary, the accuracy level of the Eclipse 8.1 plan evaluation tools are generally verified to be acceptable for use in the clinic. DVHs in the organs near high dose gradient or outside treatment beams are also recommended for further investigation.

References

1. Fraass BA, McShan DL. Three-dimensional photon beam treatment planning. In Smith AR: Radiation therapy physics. Springer-Verlag, Berlin Heidelberg, Germany, 1995:43-93.
2. Austin-Seymour MM, Chen GTY, et al. Dose volume histogram analysis for liver radiation tolerance. Int J Radiat Oncol Biol Phys.1986;12:31-5.

3. Drymala RE, Brewster L, Chu J, Goitein M, Harms W, Urie M. Dose volume histogram. Int J Radiat Oncol Biol Phys. 1991;21:71-8.
4. Lawrence TS, Tesser RJ, Ten Haken RK. An application of dose volume histogram to treatment of intrahepatic malignancies with radiation therapy. Int J Radiat Oncol Biol Phys. 1990;19:1041-7.
5. IAEA , Technical Reports Series no. 430. Commissioning and quality assurance of computerized planning system for radiation treatment of cancer. International Atomic Energy Agency, Vienna, 2004.
6. Mijnheer B, Olszewska A, Fiorino C, Hartmenn G, Knoos T, Rosenwald JC, Welleweerd H. Quality assurance of treatment planning systems. Practical examples for non-IMRT photon beams. ESTRO physics booklet no. 7 (European society for therapeutic radiation oncology), 2004
7. Panitsa E, Rosenwald JC, Kappas C. Quality control of dose histogram computation characteristics of 3D treatment planning systems. Phys Med Biol, 1998;43:2807-16.
8. Chen GTY. Dose volume histogram in treatment planning. Int J Radiat Oncol Biol Phys. 1988;14:1319-20.
9. Henríquez FC, Castrillón SV. A novel method for the evaluation of uncertainty in dose-volume histogram computation. Int J Radiat Oncol Biol Phys. 2008;70(4): 1263-71.
10. Niemierko A , Goitein M . Random sampling for evaluating treatment plans. Med Phys. 1990;17(5):753-62.
11. Lu XQ, Chin LM. Sampling techniques for the evaluation of treatment plans. Med Phys. 1993; 20(1):151-61.
12 Jackson A, Mohan R, Baldwin B. Comments on 'Sampling techniques for the evaluation of treatment plans'. Med Phys. 1993; 20(5):1375-6.
13. Niemierko A, Goitein M. Comments on 'Sampling techniques for the evaluation of treatment plans'. Med Phys. 1993;20(5):1377-80.
14. Kooy HM, Nedzi LA, Alexander E 3rd, Loeffler JS, Ledoux RJ. Dose-volume histogram computations for small intracranial volumes. Med Phys. 1993;20(3):755-60.
15. Varian Medical Systems, Inc. Eclipse treatment planning system version 8.1 customer release note.
16. Lu Wang, Jinsheng Li, Kamen Paskalev, Peter Hoban, Wei Luo, Lili Chen, Shawn McNeeley, Robert Price, and Charlie Ma. Commissioning and quality assurance on commercial stereotactic treatment-planning system for extracranial IMRT. Journal of Applied Clinical Medical Physics. 2006;7(1):21-34.

THE ASEAN JOURNAL OF RADIOLOGY 2010; 16(2): 130-138

Original Article

Abnormal Hormonal Secretions Post Radiotherapy for Nasopharyngeal Cancer*

Vimol Sukthomya, MD.

Radiology Department, Faculty of Medicine, Chiangmai University, Thailand 50200

Abstract

Objective: To investigate the incidence of abnormal hormone level in the nasopharyngeal cancer patient who received radiotherapy.

Materials and Methods: We have studied the incidence of abnormal function of adrenal and thyroid gland in patients with nasopharyngeal cancer who received radiotherapy at Division of Therapeutic Radiology and Oncology, Faculty of Medicine, Chiang Mai University. There were 60 patients, 36 male, 24 female. All patients were examined clinically and laboratory for signs of abnormal thyroid function. All patients had blood tests to determine the free hormone from thyroid and pituitary glands (TSH, FT3, FT4) and adrenal glands by using insulin tolerance test then reconfirm by using pituitary hormone injection intravenously to check the function of adrenal gland (ACTH Stimulation test).

Results: The result revealed abnormal function of adrenal glands 13.3%, abnormal thyroid function 65% in which 38.3% come from abnormality of the pituitary gland and hypothalamus (central hypothyroid) and primary hypothyroidism in 18.3%. Subclinical hyperthyroid was found in 8.3%. But we were not able to differentiate signs and symptoms of the patients with adrenal insufficiency and hypothyroidism from patients who have normal level of hormone.

Conclusion: This study found high incidence of abnormal hormone level in the nasopharyngeal cancer patient who received radiotherapy.

*Supported in part by a grant from Faculty of Medicine Chiang Mai University, Thailand

Introduction

Nasopharyngeal carcinoma is a common cancer in Southern China and Southeast Asia. In Thailand nasopharyngeal cancer is number 8 cancer found in male and it also one of the most common head and neck cancer. The standardized incidence rate of nasopharyngeal cancer in Thailand is 2.8 and 1.4 per 100,000 in males and in females respectively. Chiang Mai has the highest incidence rate of 3.8 for males and 1.6 for females.[1,2] The treatment for NPC is mainly radiotherapy or combined radiochemotherapy. The effect of radiotherapy to the normal tissue especially the thyroid gland, pituitary gland including hypothalamus may give rise to decrease hormonal level. So far we do not have the incidence of abnormal level of the hormonal in NPC patients who were treated with radiotherapy in Thailand, so this report may helps us understand the situation in this group of patients.

Materials and Methods

We have followed the patients who were treated with radiotherapy in Section of Therapeutic Radiology and Oncology, Faculty of medicine, Chiang Mai University, from 1984-1995. There were 60 patients. 36 male, 24 female age range 19-63 years, the median age for male was 47.1±11.3, and 39.9±13.2 for female.

There were 13 patient who had base of skull involvement but there was no pituitary gland involvement in all 60 patients. Last follow up C.T. scan showed no evidence of recurrent or metastases. All patients has no retreatment by radiotherapy or chemotherapy two years before the tests. Patients with convulsion, abnormality of the vessel in the brain, cardio vascular disease and other serious illness were excluded from the study.

Any patients who received the medication that may effect the testing of the hormone were asked to stop the medication for at least one month. All patients were tested for thyroid and adrenal gland functions except for one patient who did not have Insulin tolerance test due to the problem with venepuncture so ACTH stimulation was used in this patient.

All patient received one course of radiotherapy except one patient who receive first course of RT in 1987 and second course of RT for relapse in 1994.

The patients were staged according to TNM/AJCC/UICC 1986 classification, there were 2 patient in stage I, 8 patients in stage III and 50 patients in stage IV.

Radiotherapy Technique

All patients received two paralled opposing fields using Cobalt-60 or 6MV Linear Accelerator, 200 cGy/day, 5 days/week, the radiation dose was from 62-72 Gy. The treatment field covered the pituitary area and sphenoid sinuses at the upper border in all patients with stage IV, the anterior border covered the posterior 2/3 of the maxillary sinuses and in the case with anterior extension of the tumor to the nasal cavity, the field also extended to over this area, the posterior border cover the area of post auricular nodal area, the lower part of the field was at the mid part of the neck or to cover the enlarged lymphnodes area. The lower neck and supraclavicular areas were treated with anterior single field with central shielding.

After 40-44 Gy the radiation field was reduced to avoid the spinal cord. Booster dose to the enlarged lymph nodes or the area behind the cord were given by electron. The radiation dose was 50

Gy for all microscopic area, large nodes or gross tumor received higher dose to 66-70 Gy. After 60 Gy, the field was further reduced to include only nasopharyngeal area to 66-70 Gy. The anterior lower neck and supraclavicular field received 50 Gy.

Hormonal Analysis

Adrenal and Thyroid function tests were done in all patients, the tests were done 8.00AM after nothing by month at least 8 hours before the test.

Thyroid function tests

Serum thyrotropin (TSH), free triiodothyromine (FT_3) and free thyroxine (FT_4) were done by chemi-luminescent (ECLIA) by using Elecsys 1010 machine (Berringer Manheim)

The normal level for Northern Thai is

TSH = 0.32 - 4.38 /ml

FT_4 = 1.03 - 1.77 mg/dl

FT_3 = 0.22 - 0.40 mg/dl

Adrenal gland function test

Adrenal gland function test was done by insulin tolerance test (ITT), using short acting human insulin injection (Humulin - R, Eli Lilly Co.) 0.1 unit/kg then the blood was drawn for plasma glucose and cortisol at 0, 30, 60, and 90 minutes after insulin injection or more often if the patients developed any abnormal symptoms.

This test was considered completed when the level of blood sugar ≤40 mg%, if this level could not be achieve then higher dose of Insulin 0.15 - 0.2 unit/mg was given until the blood sugar level was at the above desired level. The normal ITT test was the level of serum cortisol ≥20 μ/dl during the hypoglycemia.

ACTH stimulation test was done by intravenous injection of the ACTH then the blood was drawn for cortisol level at 30 and 60 minutes, the normal value was the same as ITT.

After the blood was taken from the patients, it was immediately centrifuged and kept at -20°C, the serum cortisol was done by enzyme immuno-assay (EIA)

Statistical Method

The value of the tests were analyzed using mean and standard deviation, student's T-test was used to test the hypothesis. chi-squares and Fisher exact test were used to test the difference. The significant level is less than 0.05.

Results

The number of patients in this study were 36 males and 24 females. Mean age for male was 47.1±11.3 years and 39.9±13.2 years for female, the mean radiation dose was 70.7±5.4 Gy. Disease free interval was 55.2±34.5 months (table 1). Hypo-thyroidism occurred in 34 out of 60 patient (56.6%), 11/34 (18.3%) primary hypothyroidism, 23/60 (38.8) had central hypothyroidism and subclinical hypo-thyroidism in 5/60 (8.3%; table 3).

Adrenal insufficiency occurred in 8/60 (13.3%) patients. These patients had combined thyroid and adrenal insufficiency. One patient had hyperthyroi-dism (Table 4, 5) revealed no difference in age and radiation dose in the abnormality of the function of thyroid and adrenal glands. But female patients had significantly more abnormality of thyroid function more than male (P=0.03)

There was no difference regarding the symp-toms in the patient with normal or abnormal thyroid and adrenal gland (Table 6, 7).

Table 1 Clinical characteristics of 60 patients. thyroid and adrenal function

NO	SEX	AGE (Y)	RFI (mo.)	TD (GY)	TSH	FT4	FT3	ITT/ACTH	STAGE
1	F	31	84	76	↔	↓	↔	N	IV
2	F	24	33	70	↑	↓	↓	A	IV
2	F	42	51	70	↔	↓	↓	N	IV
4	F	40	47	66	↔	↓	↔	N	IV
5	M	32	108	70	↔	↔	↔	A	III
6	F	20	29	67	↔	↔	↔	A	IV
7	M	62	72	76	↑	↓	↔	N	IV
8	M	49	28	70	↔	↔	↔	N	IV
9	F	47	65	70	↓	↓	↓	N	IV
10	F	61	119	70	↑	↔	↓	N	IV
11	F	63	39	70	↔	↓	↔	N	IV
12	F	47	83	70	↓	↔	↔	N	IV
13	F	34	19	70	↔	↓	↓	N	IV
14	F	21	33	70	↔	↓	↓	N	IV
15	M	58	39	70	↔	↓	↓	N	IV
16	M	50	37	74	↔	↔	↔	N	IV
17	M	30	28	70	↔	↔	↔	N	IV
18	M	53	30	76	↔	↔	↔	M	IV
19	M	40	61	68	↑	↔	↔	M	IV
20	F	31	27	70	↑	↔	↔	M	IV
21	M	50	27	70	↔	↓	↓	A	IV
22	M	44	45	70	↔	↔	↔	A	IV
23	M	53	41	70	↔	↔	↓	N	IV
24	F	35	63	70	↔	↔	↔	N	IV
25	M	31	78	70	↔	↔	↔	N	IV
26	M	62	42	70	↔	↔	↓	N	IV
27	M	31	27	66	↓	↔	↔	N	IV
28	M	52	32	70	↑	↓	↑	N	IV
29	F	31	33	70	↔	↔	↔	N	IV
30	F	54	153	70	↔	↔	↔	N	I
31	M	51	120	71.4	↑	↔	↔	N	III
32	F	57	47	70	↑	↓	↔	N	IV
33	M	21	59	72	↔	↔	↓	N	IV
34	M	50	24	71.8	↔	↓	↔	N	IV
35	F	60	45	70	↑	↓	↔	N	III
36	M	62	47	70	↔	↓	↔	N	III
37	M	55	46	107	↑	↓	↔	N	IV
38	M	39	56	70	↔	↔	↔	N	IV
39	M	59	27	66	↔	↔	↔	N	III
40	M	55	24	70	↑	↓	↔	N	IV
41	M	19	30	70	↔	↓	↔	N	IV
42	F	30	22	74	↔	↓	↓	N	IV
43	M	48	120	72.5	↔	↔	↔	A	IV
44	M	55	47	70	↔	↓	↔	A	III
45	M	37	24	69	↑	↓	↔	N	IV
46	F	34	44	70	↔	↔	↔	N	IV
47	M	50	66	74	↑	↓	↓	A	IV
48	F	40	83	64	↔	↓	↔	N	IV
49	M	38	47	68	↔	↓	↓	N	IV
50	M	53	35	66	↔	↓	↔	N	IV
51	F	44	24	70	↔	↓	↓	N	IV
52	F	33	37	70	↑	↓	↓	N	IV
53	F	57	108	74.5	↑	↓	↓	N	IV
54	F	25	63	76	↔	↓	↓	A	IV
55	M	57	40	70	↔	↓	↓	N	IV
56	M	42	38	66	↔	↓	↓	N	III
57	M	60	47	70	↔	↓	↓	N	IV
58	M	41	80	65	↔	↓	↓	N	IV
59	M	54	95	70				N	III
60	M	49	192	66				N	IV
MEAN	44.2	55.2	70.7					N	I
SD	12.5	34.5	5.4						

RFI = Radiation free interval TD = Total dose ACTH = ACTH stimulation test

ITT = Insulin tolerance test N or ↔ = Normal, ↓ = Decrease, ↑ = increase, A = Abnormal.

F = Female M = Male

Table 2 Incidence of Hypothyroidism

Abnormal	Male	Female	Total (%)
Primary hypothyroid	5	6	11 (18.3)
Central hypothyroid	12	11	23 (38.3)
Subclinical hypothyroid	2	3	5 (8.3)

Table 3 Incidence of Adrenal insufficiency

Abnormal	Male	Female	Total (%)
Adrenal insufficiency	5	3	8 (13.3)

Table 4 Characteristics of the patients with abnormal thyroid function

	Abnormal	Normal	Significant
Male	19	17	Significant
Female	20	4	(P=0.03)
Mean age (year)	43.3±13.1	45.9±11.4	NS
Radiation free interval (month)	55.9±34.2	53.9±35.9	NS
Radiation dose (Gy)	70.9±6.5	70.3±2.4	NS

Table 5 Chracteristics of the patients with abnormal adrenal function

	Abnormal	Normal	Significant
Male	5	31	Significant
Female	3	21	(P=0.82)
Mean age (year)	42.0±14.5	44.6±12.3	NS
Radiation free interval (month)	67.3±39.2	53.3±33.8	NS
Radiation dose	71.0±2.5	70.7±5.8	NS

Table 6 Relationship of symptoms and adrenal gland function

Symptoms	Abnormal hormone (%)	Normal hormone (%)
Weakness	12.5	15.4
Fatique	12.5	19.2
Anorexia	12.5	7.7
Joint pain	12.5	3.9
Postural dizziness	37.5	9.6

Table 7 Relationships of symptoms and thyroid function

Symptoms	Abnormal hormone (%)	Normal hormone (%)
Decrease sweating	17.9	9.5
Cold intolerance	35.9	28.6
Decrease hearing	25.6	33.3
Hoarseness	20.5	4.8
Weight gain	12.8	4.8
Constipation	12.8	14.3
Muscle cramp	12.8	0
Paresthesia	7.7	4.8
Slow reflex relaxation	15.4	9.5

Discussion

After radiotherapy to the brain, abnormality of hypothalamic pituitary function has been reported [3-12]. Several reports also revealed symptomatic hypopituitarism in nasopharyngeal patients after receiving radiotherapy for 2-5 year[13,14].

Lam et al.[14] studied the function of pituitary gland and hypothalamus in 31 patients, the dose of radiation to pituitary gland and hypothalamus was 3,979±78 Gy and 6,167±100 cGy. After five years post radiotherapy, there were significant abnormal secretion of growth hormone 63.5%, gonadotropine 30.7%, corticotropine 26.7% and thyrothropine 14.9%.

Turner et al.[15] reported 32 patients with brain tumor who were followed for 2-13 years after received radiotherapy from 3,960 to 7,020 cGy. Most of the patients had abnormality of the function of pituitary and hypothalamus. The most frequent findings was gonadal dysfunction 61%, hypothyroid 28% and mild abnormality of the function of adrenal gland.

Our study in the nasopharyngeal cancer patients who were followed for at least two years and were without evidence of disease. There were evidence of abnormality in the secretion of thyroid glands (primary hypothyroid, secondary hypothyroid and subclinical hypothyroid) which was found in 65%, constituted primary hypothyroid 18.3%, central hypothyroid 38.3% and subclinical hypothyroid 8.3%. Abnormal of the function of adrenal glands was found in 13.3%.

Tunbridge et al.[16] reported the frequency of hypothyroid in general population of England, there were 1.9% incidence in female and 0.1% in male. Other report[17-21] found almost the same incidence with 2% in female an d 0.13% in male.

Our study revealed much higher incidence of hypothyroidism than normal incidence in general population. Hypothyroidism was found in 52.8% and 83.3% in male and female patients with nasopharyngeal cancer who received radiotherapy. Symptoms and signs are not predictor for hypothyroidism because there were no different in symptoms and signs for those patients with normal blood tests comparing to the groups with hypothyroidism.

Many reports revealed the incidence of 2.5-10.4% for subclinical hypothyroid[17-27]. Arem et al.[18]

reported the study from Japan in the study of the patients >40 years old, they found 3.2% incidence of subclinical hypothyroid for male and 5.5% for female. Our study found 8.3% of subclinical hypothyroidism, 40% in male and 60 % in female.

In this study, some of the patient also received chemotherapy, mainly cisplatin based during or after radiotherapy However, the effect of chemotherapy on thyroid glands has not been reported.[19-21]

The mechanism of abnormality of the function of the thyroid gland possibly due to follicle cells and vascular damages by radiation dose as low as 2.25 Gy[28]. The damage is not only involving the capillary but also fibrosis of thyroid capsule so the thyroid can not increase in size in order to meet the demand of the body resulting in hypothyroidism[29]. There is a report that radiation to the neck area may cause arteriosclerosis which in theory may effect the small arteries from the carotid especially superior thyroid artery[30]. There is also a report of increasing thyroid antibody after radiation to the neck[31]. In the patients who have mild thyroiditis, they may be more sensitive to thyroid antibody after radiation to the thyroid.

Central hypothyroid may occur from radiation given to the pituitary gland and/or hypothalamus. If the patients develops primary hypothyroid in which free T_4 is low and marked decrease in total T_4. The patient may develop central hypothyroid in which both free T_4 and total T_4 is low accompany with normal TSH, or slighter lower or higher TSH. All these patients should be treated with 25-200 µgram/day. But in the patient with severe hypothyroid should be treated with 100-150 µgram/day.

There are some controversy regarding treating the patient with subclinical hypothyroid who has high serum TSH but T_4 is normal. In general, we should start treating those patient with high TSH who also has abnormal symptoms or in the case of TSH over 10 µu/ml with increase antithyroid antibody because these patients may progress to develop overt hypothyroid.

There is no clear evidence that for patients who develop subclinical hypothyroid from radiation progress to overt hypothyroid. There is a report[17] revealed that the patients who receive radiation to the head and neck area developed 95% subclinical hypothyroid and 14.3% clinical hypothyroid. After 5-year follow up, clinical hypothyroid has increase to 40%. If this is the case, treatment for subclinical hypothyroid in this situation is reasonable as in the case of increase thyroid antibody.

There were some evidence that radiation in the animal to the thyroid developed increase TSH later on, may have increase risk of thyroid cancer. Patients with nasopharyngeal cancer who may live without disease for a long time may have a high risk of developing thyroid cancer so thyroid hormone may be necessary for these patients to bring down the TSH level in order to prevent thyroid cancer. So regular check up of the function of the thyroid may help identify the patient with subclinical disease.

It should be noted that the TSH in some patients with primary hypothyroid in this study was not as high as in the theory. Because in theory the relationship between the level of FT_4 and TSH is inverse proportion and it is log linear relation for example if the FT_4 level decrease 50%, the TSH increase 90 fold as 9,000% these patients may also have central hypothyroid in additional to primary hypothyroid.

Secondary adrenal insufficiency may also occur from radiation to pituitary gland or hypothala-

mus. In this study, adrenal insufficiency developed in 13.3%. The symptoms of adrenal insufficiency were not clearly shown in these patients.

In summary, because of the frequent development of the abnormality of the function of the thyroid and adrenal gland, the patients who receive radiation to the head and neck area should have endocrine assessment at 3 months post radiation and yearly thereafter.

References

1. Chiang Mai Cancer Registry. Annual Report 2006.
2. Khuhaprema T, Srivatanakul P, Sriplung H, Wiangnon S, Sumitsawan Y, Attasara P. Cancer in Thailand 1998-2000. Vol.IV. Bangkok Edical Publisher, 2007.
3. Bhandare N, Kennedy L, Morris G, Malyapa R, Mendenhall WM. Hypopituitarism after radiation therapy for extracranial head and neck cancers. Int J Radiat Oncol Biol Phys 2006;66(3):5187.
4. Blatt J, Lee P, Suttner J, Finegold D. Pulsatile growth hormone secretion in children with acute lymphoblastic leukemia after 1800 cGy cranial irradiation. Int J Radiat Oncol Biol Phys 1988;15:1001-6.
5. Constine LS, Woolf PD, Cann D. Hypothalamic-pituitary dysfunction after radiation for brain tumors. N Engl J Med 1993;328:87-94.
6. Fernandez A, Brada M, Zabuliene L, Karavitaki N, Wass J. Radiation-induced hypopituitarism. Endocrine-Related Cancer 2009;16(3):733-72.
7. Gleeson HK, Shalet SM. The impact of cancer therapy on the endocrine system is survivors of childhood brain tumours. Endocrine-Related Cancer 2004;11(4):589-602.
8. Littley MD, Shalet SM,Beardwell CG. Hypopituitarism following external radiotherapy for pituitary tumor in adults. Q J Med 1989;262:145-60.
9. Pomarede R, Czernichow P, Zucker JM. Incidence of anterior pituitary deficiency after radiotherapy at an early age: study in retinoblastoma. Acta Pediatr Scand 1984;73: 115-9.
10. Samaan NA, Schultz PN, Yand KP. Endocrine complications after radiotherapy for tumors of head and neck. J lab clin Med 1987;38:364-72.
11. Shalet SM, Beardwell CG, Morris-Jones PH, Pearson D. Pituitary function after treatment of intracranial tumor in children. Lancet 1975;2:104-7.
12. Yuen K, Cook D, Ong K, Chatelain P, Frykund L, Gluckman P, et al. The metabolic effects of short-term administration of physiological versus high doses of GH therapy in GH deficient adults. Clinical Endocrinology 2002;57:333-41.
13. Yoon SC, Suh TS, Jang HS, Chung SM, Kim YS, Ryu MR, et al. Clinical results of 24 pituitary macroadenomas with linac-based stereotactic radiotherapy. International Journal of Radiation Oncology, Biology, Physics 1998;41:849-53.
14. Lam KSL, Tse VK, Wang C. Effect of cranial irradiation on hypothalamic-pituitary function: 5-year longitudinal study in patients with nasopharyngeal carcinoma. Q J Med 1991:78:165-76.
15. Turner SL, Tiver KW. Thyroid dysfunction following radiotherapy for head and neck cancer. Int J Radiat Oncol Biol Phys 1995;31:279-90.
16. Tunbridge WMG, Evered DC, Hall R. The spectrum of thyroid disease in a community: The whickham survey. Clin Endocrinol 1977;7:481.
17. Helfand M, Bengtsson C, Lindquist O. Thyroid disease and high concentration of serum thyrotropin in a population sample of women. Acta Med Scand 1981;210:39-46.
18. Arem R, Escalante D. Subclinical hypothyroidism: epidemiology, diagnosis, and significance. Adv intern med 1996; 41:213-37.
19. Grande C. Hypothyroidism following radiotherapy for head and neck cancer: multivariate analysis of risk factors. Radiother Oncol 1992;25:31-6.
20. Posner MR, Ervin TJ, Fabian RL. Incidence of hypothyroidism following multimodality treatment for advanced squamous cell cancer of the head and neck. Laryngoscope 1984;94:451-4.
21. Ponsner MR, Weichselbaum RR, Fitzgerald JJ. Treatment complications after sequential combination chemotherapy and radiotherapy with or without surgery in previously untreated squamous cell carcinoma of the head and neck. Int J Radiat Oncol Biol Phys 1985;11:1887-93.
22. Alterio D, Jereczek-Fosssa B,Franchi B, D'Onofrio A, Piazzi V, Rondi E, et al. Thyroid disorders in patients treated with radiotherapy for head and neck cancer: A retrospective analysis of seventy-three patients. Int J Radiat Oncol Biol Phys 2007;67(1):144-50.

23. Bhandare N, Kennedy L, Malyapa R, Morris CG, Mendenhall WM. Primary and central hypothyroidism after radiotherapy for head and neck tumor. Int. J Radiat Oncol Biol Phys 2007;68(4):1131-9.

24. Diaz R, Jaboin JJ, Morales-Paliza M, Koehler E, Phillips JG, Stinson S, et al. Hypothyroidism as a consequence of intensity-modulated radiotherapy with concurrent taxane-based chemotherapy for locally advanced head and neck cancer. Int J Radiat Oncol Biol Phys 2009;75: 1-9.

25. Tell R, Lundell G, Nilsson B, Sjodin H, Lewin F, Lewensohn R. Long-term incidence of hypothyroidism after radiotherapy in patients with head and neck cancer. Int J Radiat Oncol Biol Phys 2004;60(2):395-400.

26. Wu YH, Wang HM, Chen HHW, Lin CY, Chen EYC, Fan KH, et al. Hypothyroidism after radiotherapy for nasopharyngeal cancer patients. Int J Radiat Oncol Biol Phys 2010;76(4):1133-9.

27. Sukthomya V, Sukthomya C. Thyroid dysfunction following external radiation for head and neck cancer. Thai J radio 1988;24:71-4.

28. Palmer BB, Gaggar N, Shaw HJ. Thyroid function after radiotherapy and laryngectomy for carcinoma of the larynx. Head and Neck Surg 1981;4:13-5.

29. Howes EL, Suoy JW, Harvey SC. The healing for wounds as determined by their tensite strength. JAMA 1929;92: 42-95.

30. Feehs RS, McQuirt WT, Bond MG. Irradiation: A significant factor for carotic artherosclerosis. Arch Otolaryngol Head and Neck Surg 1991;117:1135-7.

31. Markson JL, Flatman GE. Myxedema after deep x-ray therapy to the neck. South Med J 1965;1:1228-30.

THE ASEAN JOURNAL OF RADIOLOGY 2010; 16(2): 139-143 139

Case Report

FDG PET/CT in Patient with Brain Metastasis from Cervical Carcinoma: A Case Report

Pawana Pusuwan, MD.[1], Yaowalak Chansilpa, MD.[2], Orasa Chawalparit, MD.[3]

[1] *Division of Nuclear Medicine, Department of Radiology, Faculty of Medicine Siriraj Hospital, Mahidol University*

[2] *Division of Radiotherapy, Department of Radiology, Faculty of Medicine Siriraj Hospital, Mahidol University*

[3] *Division of Diagnostic Radiology, Department of Radiology, Faculty of Medicine Siriraj Hospital, Mahidol University*

Abstract

Central nervous system involvement by cervical cancer is uncommon. We report a rare case of cerebral metastasis from cervical carcinoma which was demonstrated on FDG PET/CT. The prior routine MRI brain study showed no evidence of metastasis. Apart from cerebral metastasis, PET/CT also showed multiple sub-centimeter hypermetabolic nodules in both lungs with metastatic nodes involving the right hilar and sub-carinal region. Whole body PET/CT may be helpful not only to localize the lesion in the brain but also to demonstrate other unsuspected metastatic lesions.

Keywords: Brain metastasis; Central nervous system metastasis; Cervical cancer

Introduction

MRI is the most sensitive test for detecting brain metastasis as it is superior to both CT scan and FDG PET for this purpose.[1,2] One study comparing PET scans to MRI showed that PET scans detected only 61% of the lesions detected by MRI.[3] FDG PET imaging is less sensitive for detecting brain metastases due to the high metabolic rate within the normal grey matter and variable FDG accumulation is reported in a few metastatic lesions.[2,4,5] We report a case of omission of brain metastasis by routine MRI that were later identified by PET/CT.

Case report

A 82-year-old female with initially diagnosed with stage-IIB squamous cell carcinoma of the cervix. An abdominal and pelvic CT scan revealed heterogeneous enhancing cervical mass sized 5x7 cm in diameter with a small pulmonary nodule (sized 5 mm) at anterior basal segment of RLL. A chest CT imaging showed a small nodule at each lung base (sized 5 mm and 4.5 mm) that was too small to identify the cause. She was treated with whole pelvis irradiation and high dose radiation therapy. She had a good clinical response after treatment.

Four months after treatment, she presented with back pain. Bone scan showed multiple bone metastases at left frontal and parietal bone, base of skull, left scapula, left acromioclavicular joint, anterior end of left 6th rib and multiple levels of lumbar spines. At the same time, she also had left strabismus. MRI brain showed generalized brain atrophy with secondary ventricular dilatation. No evidence of metastasis (Figure 1). Whole body PET/CT performed 1 week later showed hypermetabolic metastatic lesions at left cavernous sinus and middle cranial fossa most likely from metastatic lesions (Figure 2). Apart from multiple hypermetabolic bone metastases, multiple sub-centimeter hypermetabolic metastatic nodules were noted in both lungs with metastatic lymph nodes involving right hilar and subcarinal area (Figure 3). Retrospectively, the source image of MRA (thin slice ~0.7-1 mm) showed the mass posterior to the left cavernous sinus displaced the left internal carotid artery anteriorly (Figure 4). She was treated by two-opposing views irradiation.

Discussion

Metastatic lesion is the most common mass lesions in the brain with the reported primary sources from lung, breast, malignant melanoma, kidney and gastrointestinal tract cancers.[6] Brain metastasis from cervical cancer is very rare with reported incidence of 0.5% to 1.2%.[7] The most common reported symptoms and signs in brain metastasis are headache and hemiparesis.[7] The presenting symptom in our patient was left strabismus as the lesion was located in the left cavernous sinus.

FDG PET has been accepted as a useful tool for oncologic staging in several types of cancer.[8] Rohren et al recommended not to routinely perform scanning of the brain in patients undergoing whole-body FDG PET for staging of non-CNS malignancy.[3] The reason of the limited use of FDG PET in brain imaging is due to the high metabolic rate within the grey matter.[4] This case serves to illustrate that FDG PET/CT scan is useful to detect metastatic brain lesion and also other unsuspected metastatic lesions.

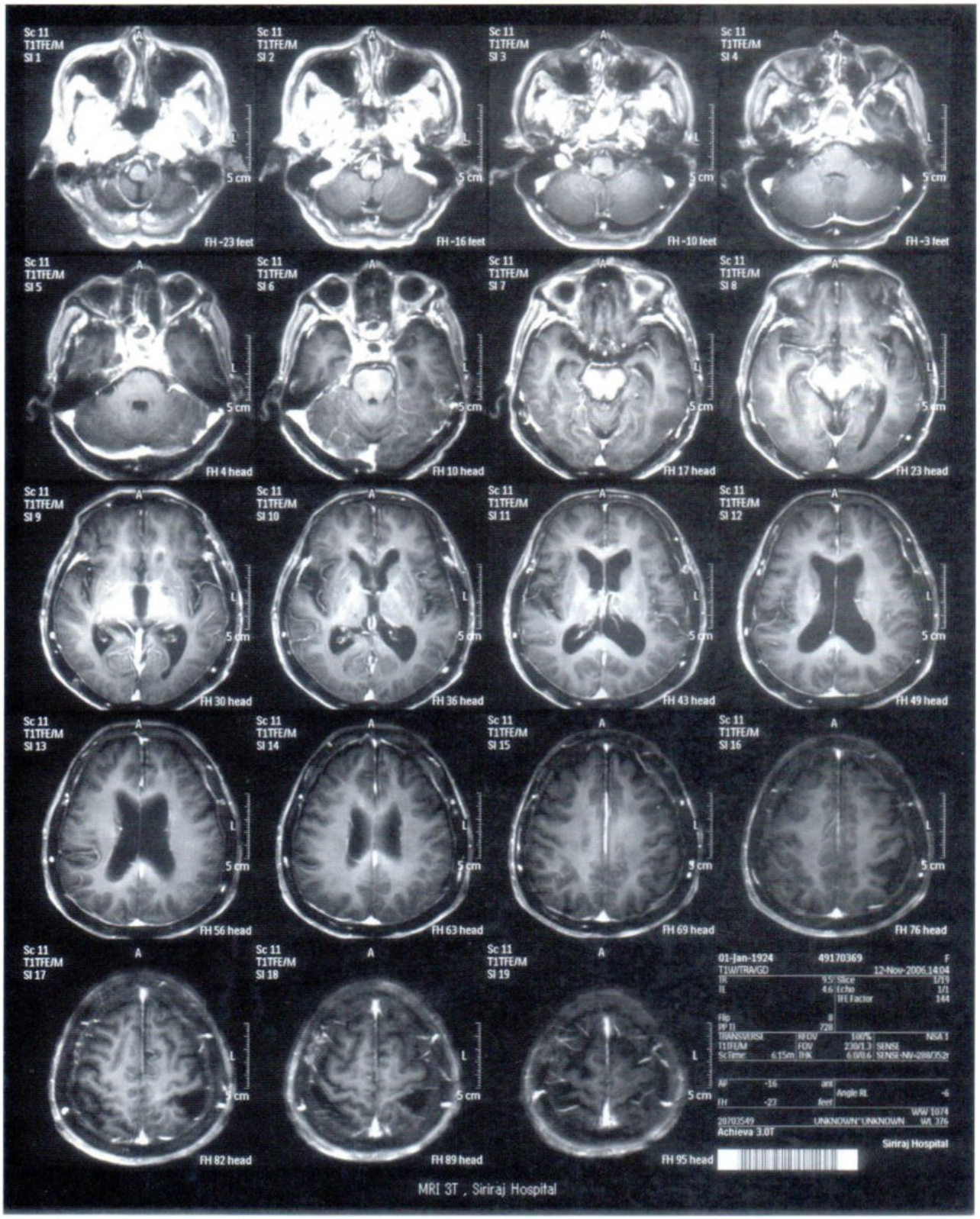

Fig.1 MRI brain shows generalized brain atrophy with secondary ventricular dilatation. No evidence of metastasis.

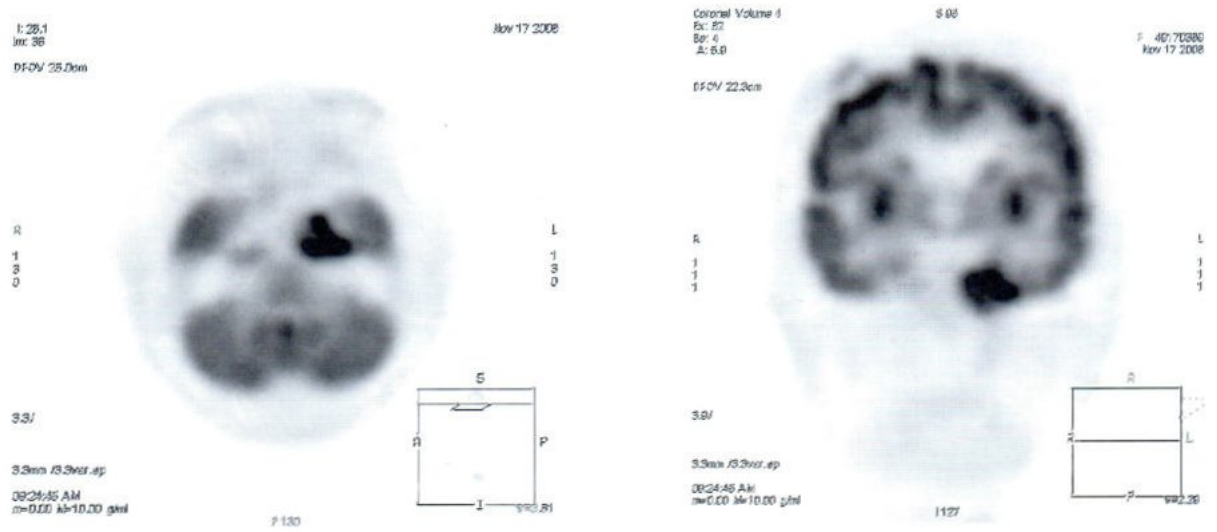

Fig.2 Transaxial and coronal PET scan show hypermetabolic metastatic lesion at left cavernous sinus and middle cranial fossa.

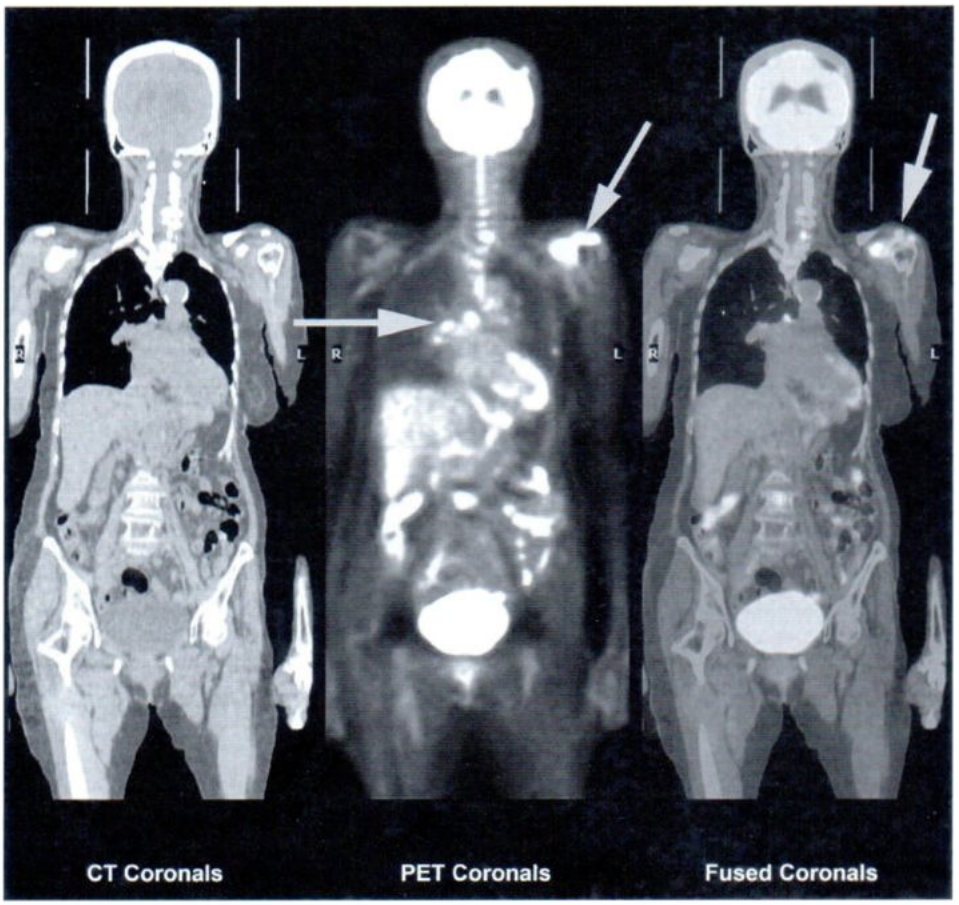

Fig.3 Coronal PET/CT scan shows multiple metastatic lesions at left scapula, right hilar and subcarinal nodes.

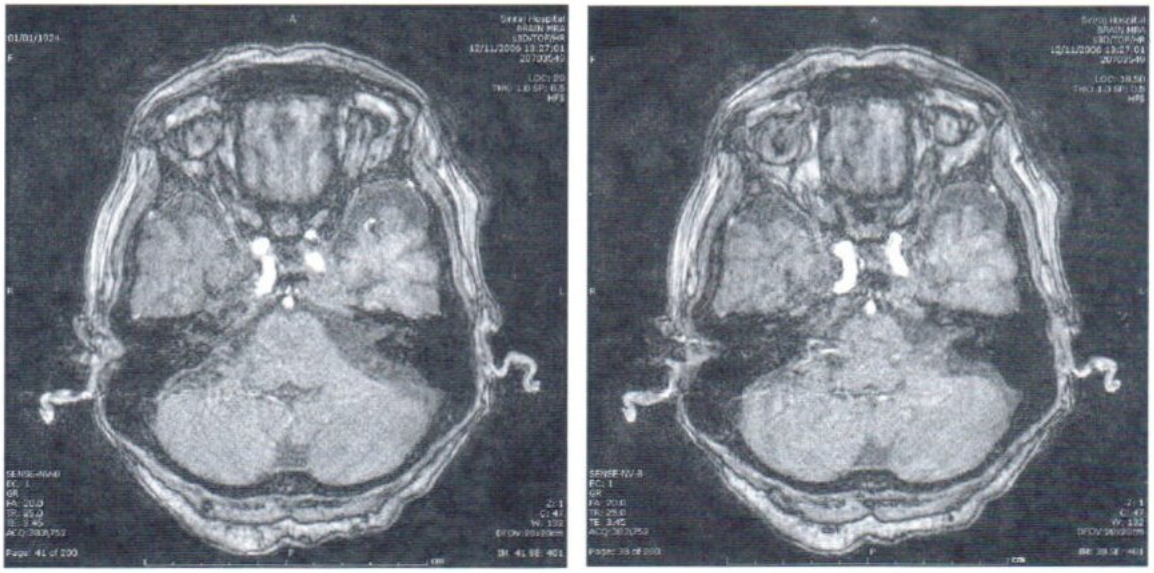

Fig.4 The source image of MRA (thin slice 0.7-1 mm) shows mass at posterior left cavernous sinus. The left internal carotid artery is displaced anteriorly.

References

1. Yokoi K, Kamiya N, Natsuguma H, et al. Detection of brain metastasis in potentially operable non-small lung cancer: a comparison of CT and MRI. Chest 1999;115: 714-9.
2. Kuhlman JE, Perlman SB, Weigel T, et al. PET scan-CT correlation: what the chest radiologist needs to know. Curr Probl Diagn Radiol 2004;33:171-88.
3. Rohren EM, Provenzale JM, Barboriak DP, et al. Screening for cerebral metastases with FDG PET in patients undergoing whole-body staging of non-central nervous system malignancy. Radiology 2003;226:181-7.
4. Lira A. Brain cancers. In: Alazraki NP, Shumate MJ and Kooby DA. A clinician's guide to nuclear oncology. The Society of Nuclear Medicine, Reston: 2007;161-9.
5. Hagge RJ, Coleman RE. Positron emission tomography: lung cancer. Semin Roentgenol 2002;37:110-7.
6. Gupta NC, Nicholson P, Bloomfield SM. PDG-PET in the staging work-up of patients with suspected intracranial metastatic tumors. Ann Surg 1999;230:202-6.
7. Amita M, Sudeep G, Rekha W, et al. Brain metastasis from cervical carcinoma-A case report. Medscape General Medicine 2005; 7: 26. Available at www.medscape.com/viewarticle/496603. Accessed August 5, 2008.
8. Gambhir SS, Czermin J, Schwimmer J, et al. A tabulated summary of the FDG PET literature. J Nucl Med 2001; 42(5 Suppl.):1S-93S.

THE ASEAN JOURNAL OF RADIOLOGY 2010; 16(2): 144-146

Case Report

Increased Muscle Uptake of Bone Seeking Agent in A Patient with Polymyositis: A Case Report

Pawana Pusuwan, MD.

Division of Nuclear Medicine, Department of Radiology, Faculty of Medicine Siriraj Hospital, Mahidol University, Bangkoknoi, Bangkok 10700, Thailand.

Abstract

A 38-year-old male presented with fever, muscle pain, weakness and acute renal failure. Tc-99m methylene diphosphonate (MDP) bone scan showed increase uptake by muscles of the shoulders and hips. Biopsy of the deltoid muscle was compatible with myositis. On two consecutive follow-up scans, the degree of muscle uptake correlated well with the recovery of the disease.

Keywords: Bone scan; polymyositis; acute renal failure

Introduction

Tc-99m MDP bone scan, introduced by Subramanian and McAfee[1] in 1971, has become one of the most widely used investigations in nuclear medicine for a variety of benign and malignant skeletal conditions[1]. The major mechanism of the tracer binding into the skeleton is chemisorption. Soft tissue uptake is an uncommon finding on bone scan.

Case Report

A 38-year-old male presented with progressive 5 weeks history of fever, pain and weakness in his proximal upper and lower extremities. Seven days before admission he had a difficulty in walking with swelling legs. There was no previous history of strenuous exercise or using alcohol or drugs. He had no family history of neuromuscular disorder.

Upon admission, laboratory values showed a serum BUN of 194 mg/dl, serum creatinine of 10.9 mg/dl, serum creatinine phosphokinase (CPK) of 49,506 U, calcium 4.5 mg/dl and phosphate 12 mg/dl. A Tc-99m MDP bone scan demonstrated increased radioactivity uptake in various muscles at bilateral shoulders and hips. Increased uptake in bilateral enlarged kidneys was noted (Fig.1). Small amount of faint activity in the urinary bladder was seen. Biopsy of the deltoid muscle was compatible with myositis. Acute renal failure from polymyositis with rhabdomyolysis was most likely.

After steroid therapy with hemodialysis, the patient's renal impairment and muscle strength gradually improved. Follow-up bone scan 2 weeks later showed only small amount of muscle uptake persistence at bilateral shoulders and hips (Fig.2). The last bone scan done one month later appeared unremarkable.

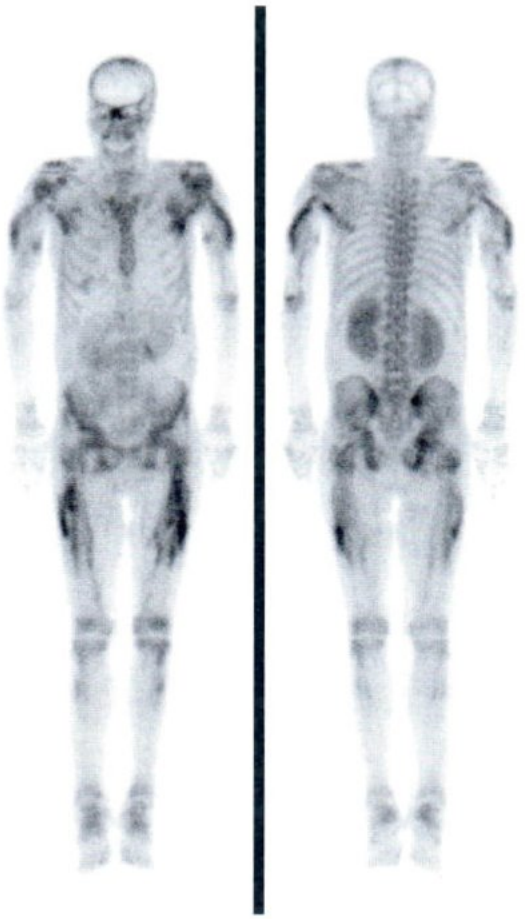

Fig.1 Tc-99m MDP bone scan shows increased radioactivity uptake in the muscles of shoulders and hips.

Discussion

Bone scan provides very sensitive information about the abnormalities of bone physiology. The most frequent nonosseous uptake on bone scan is related to the urinary system[2]. Other nonbony structures can be demonstrated on the bone scan. The recognition of these extraosseous uptake is important for accurate interpretation of the scan although the main purpose of the study is to address the skeletal abnormalities.

The presence of diffuse skeletal muscle uptake on bone scan is rare. Increased uptake in

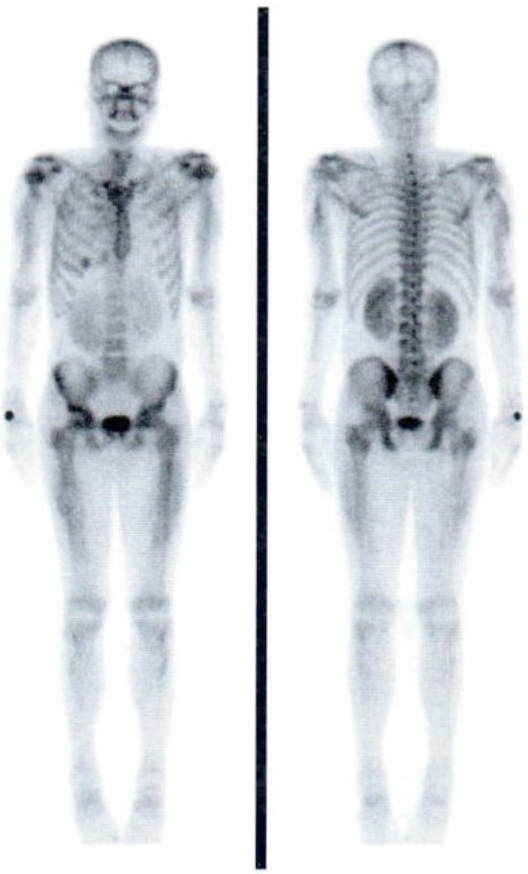

Fig.2 Follow-up bone scan 2 weeks after the first study shows diminished radioactivity uptake in the muscles.

the muscles of shoulders and hips with the clinical symptoms of muscle pain and weakness in this case lead to the suspicious of polymyositis which was confirmed by muscle biopsy. Polymyosistis is reported as one of the principle cause for muscle uptake on bone scan[3-5]. It is a rare autoimmune disease characterized by progressive muscle inflammation. This illness can lead to symmetric proximal muscle weakness of the extremities and severe disability. Spies DM, et al reported the first case of Tc-99m phosphate uptake in inflammatory muscle disease[6]. Other reported causes include rhabdomyolysis, dermatomyositis, muscular dystrophy, amyloidosis, overexertion, HIV-associated myositis, paraneoplastic syndrome and uremic myositis[7].

Tc-99m MDP bone scan in a patient suspicious of polymyositis may be useful to confirm the diagnosis of inflammatory muscle and also localize the appropriate site for muscle biopsy.

References

1. Subramanian G, MacAfee JG. A new complex of 99mTc for skeletal imaging. Radiology 1971;99:192-6.
2. Loutfi I, Collier D, Mohammed AM. Nonosseous abnormalities on bone scan. J Nucl Med Tech 2003;31:149-53.
3. Yonker RA, Webster EM, Edwards NL, Katz P, Longley S, Petersen H, et al. Technetium pyrophosphate muscle scans in inflammatory muscle disease. British J of Rheumatology 1987;26:267-9.
4. Kim HW, Choi JR, Jang SJ, Chang YS, Bang BK, Park CW. Recurrent rhabdomyolysis and myoglobinuric acute renal failure in a patient with polymyositis. Nephrol Dial Transplant 2005;20:2255-8.
5. Niemir Z, Oleksa R, Czepczynski R, Sowinski J. Increased uptake of technetium-99m methylene diphosphonate in muscles in the course of polymyositis. Nucl Med Review 2005;8:153-4.
6. Spies SM, Swift TR, Brown M. Increased technetium-99m polyphosphate muscle uptake in a patient with polymyositis. J Nucl Med 1975;16:1125-7.
7. Datz FL. Gamuts in nuclear medicine (3rd edn). Mosby-Year Book, Inc. 1995.

Instructions for Authors

1. The Asean Journal of Radiology publishes the papers on Radiological Sciences, such as research work, reviews articles case reports, innovations in medical Sciences related to all branches of Radiology, and letters to the editor. The aforementioned materials can be written in English only.
2. The authors have to submit 2 copies of the manuscript and a CD :to Assoc. Prof. Sirintara Singhara Na Ayudya, Department of Radiology, Faculty of medicine, Ramathibodi hospital 270, Rama VI Road, Toong Phayathai, Ratchathewi, Bangkok, 10400. Tel 02-2011259#110, Fax 02-2011297, E-mail Sirintarapongpech2@hotmail.com
3. The original copy to be submitted must be typed in a double space on one of the page 8.5"x11" (A4) paper.
4. The format of the article must include:
   a. Title page and address of the author (s)
   b. Abstract (Objective, Methods, Results and conclusion)
   c. Introduction
   d. Material and Method
   e. Results and discussion
   f. Acknowledgment (if any)
   g. References (Follow the Vancouver style)
5. We will provide 5 copies of reprints for the author (s) an article for publication in the Asean Journal.
6. The illustrations and table must be clearly prepared with legends in English as they are the art works to be reproduced
7. The authors are responsible for the contents of the article as to its facts and findings.
8. Ethics

Paper reporting studies which might be interpreted as human experimentation (e.g. controlled trials) should conform to the standards of the Declaration of Hilsinki (see British Medical Journal 1964:2:177) and should indicate that, approval that such studies may proceed, has been granted by the local or hospital Ethics Committee.

When reporting experiments on animal indicate whether the institution's or the National Research Council's guide for, or any national law on, the care and use of laboratory animals was followed.

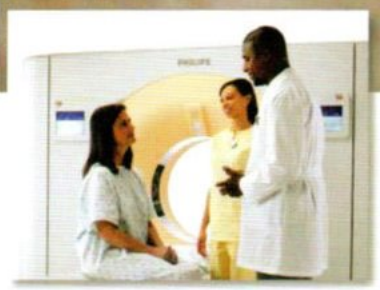

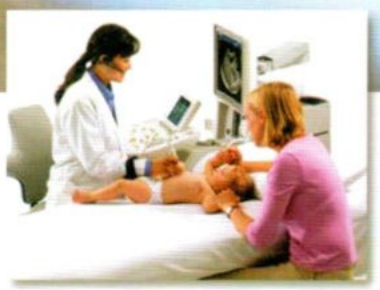

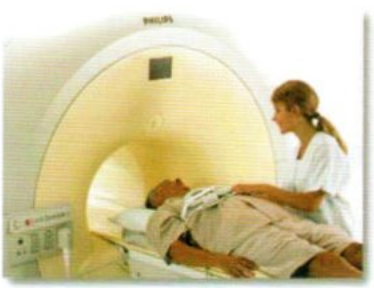

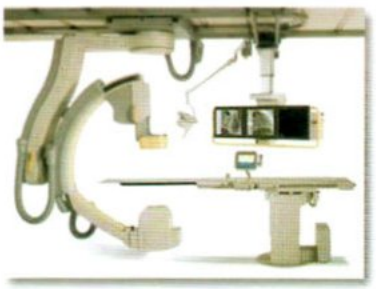

Philips Electronics (Thailand) Ltd.
28th floor, Thai Summit Tower New Petchburi Road,
Khwaeng Bangkapi Khet Huaykhwang Bangkok 10310
Tel. 02-614 3440 Fax. 02-614 3562
www.philips.com

PHILIPS
sense and simplicity